UNITED STATES DEPARTMENT OF THE INTERIOR

GEOLOGICAL SURVEY

Fluid-inclusion data on samples from Creede, Colorado, in relation to mineral paragenesis

By

Terri L. Woods, Edwin Roedder, and Philip M. Bethke

Open-File Report 82-313

1982

CONTENTS

ILLUSTRATIONS

TABLES

Abstract

Published and unpublished data on 2575 fluid inclusions in ore and gangue minerals from the Creede, Colorado, Ag-Pb-Zn-Cu vein deposit collected in our laboratories from 1959 to 1981 have shown that the average salinity (wt. % NaCl equivalent, hereinafter termed wt.% eq.) and homogenization temperature (Th), and the ranges of these two parameters for fluid inclusions in sphalerite, quartz, fluorite, and rhodochrosite, respectively, are 8.1 (4.6 - 13.4), 239°C (195-274°C); 6.1 (1.1-10.0), 260°C (190->400°C); 10.7 (6.1-11.1), 217°C (213-229°C) and 260°C (247-268°C) (bimodal distribution of Th); and 9.9 (9.3 - 10.6), 214°C (185-249°C). Inclusions have been measured in minerals from four of the five stages of mineralization previously recognized at Creede. The few inclusions of fluids depositing rhodochrosite (A-stage, earliest in the paragenesis) yield Th and salinity values more similar to those of the low-temperature (average Th 217°C) fluids forming some of the much later fluorite (C-stage) than to any of the other fluids. Th measurements on A-stage quartz range from 192°C to 263°C and average 237°C. The early, fine-grained, B-stage sphalerites yielded Th of 214 to 241°C and salinities of 6.1 to 10.2 wt. % eq.

D-stage sphalerite (late in the paragenesis) has been studied in detail (growth-zone by growth-zone) for several localities along the OH vein and reveals a generally positive correlation among Th, salinity and iron content of the host sphalerite. The deposition of D-stage sphalerite was characterized by repeated cycling through different regions of salinity/Th space, as Th and salinity generally decreased with time. Seventeen salinity-Th measurements were made on D-stage sphalerite from one locality on the Bulldog Mountain vein system, which, like the OH vein, is one of four major ore-producing vein systems at Creede. These data suggest a lower Th for a given salinity fluid from sphalerite on the Bulldog Mountain vein than on the OH vein. The very high values of Th for some quartz samples (mostly D-stage) are believed to be a result of the trapping of both gas and liquid from a boiling fluid in the upper levels of the vein system. Boiling of fluids depositing D-stage quartz is indicated by the presence of steam inclusions in quartz and the extreme variability of Th values measured on quartz. The pressure was low ($\leq$ 125 kg/cm^2) throughout ore deposition.

Three major growth zones in D-stage sphalerite are recognized throughout the OH vein. Deposition of the first major zone began from fluids having intermediate salinities and temperatures (7.8-9.2 wt. % eq., 240°C) but the characteristics of the fluids oscillated after that, ranging from 7.2 to 10.1 wt. % eq. and from 225°C to 270°C. Deposition of the second major, most Fe-rich zone began with the hottest, most saline fluids present during D-stage mineralization (270°C, 10.5-12.5 wt. % eq., 3 mole % FeS in sphalerite). The fluid then oscillated with respect to Th and salinity (213-274°C, 5.2-12.5 wt. % eq.) but showed a general decrease in both with time. Deposition of the youngest major zone began with a very Fe-poor sphalerite (0.25-0.75 mole % FeS), from the least saline, coolest fluids (5-6.5 wt. % eq., 200-212°C) and ended with a trend of increasing temperature at approximately constant salinity.

The fluid-inclusion data can best be explained by a mixing model involving at least two fluids--one hot and saline, the other cool and fresher. Sudden changes in the mixing ratio, presumably from changes in the plumbing, punctuated long periods of remarkably uniform conditions of ore fluid flow and deposition. The effects of other processes such as convection and heat exchange with wall rocks must have been superimposed on this simple mixing model, however. In contrast to an earlier interpretation, several aspects of the inclusion data may be interpreted to suggest exceedingly slow ore deposition. Work in progress may resolve some of these ambiguities and refine the model.

INTRODUCTION

From 1959 to 1981, fluid inclusions in ore and gangue minerals from the Creede, Colorado, Ag-Pb-Zn-Cu epithermal vein deposit have been studied in a number of ways and for a variety of purposes. Some of the data gathered in these studies have been published in widely scattered articles (see table 2); other data have been presented in summary form only, and a large number of homogenization and salinity measurements have never been published. In this report, we summarize the earlier published reports, present the remaining unpublished data, make some tentative interpretations of the data in the light of companion studies of other aspects of the Creede district, and, finally, outline the systematic investigation of the thermal, chemical and isotopic evolution of the Creede ore fluids that is currently underway in our laboratories. In all, data are presented herein from the observation and measurement of 2575 individual inclusions in five phases from 61 sample localities, 57 of which are on the OH vein.

GEOLOGIC SETTING

A brief summary of the geologic setting of the Creede district is included below to save reference to the many previous publications from which it has been drawn. The volcanic stratigraphy of the central San Juan Mountains is summarized in table 1.

Mineralization at Creede appears to have been the latest event in a sequence of Middle Tertiary volcanism and related activity which began in earliest Oligocene time, approximately 40 million years ago, with the eruption of intermediate composition lavas from a large number of volcanic centers. These lavas and associated volcaniclastic fans coalesced to form a continuous volcanic cover averaging about 1 km in thickness over most of the area of the present southern Rocky Mountains (Steven and Lipman, 1976). Between 30 and 26 1/2 million years ago, a major batholith worked its way up to shallow depths below the San Juan volcanic field, resulting in widespread ash-flow-tuff extrusion and related caldera subsidences (Plouff and Pakiser, 1972). The Bachelor caldera, the second caldera of seven formed between approximately 28 and 26 1/2 million years ago in the immediate vicinity of the Creede district (fig. 1), was the source of the Carpenter Ridge Tuff, which hosts most of the Creede veins (Steven and Eaton, 1975). Resurgent doming of the Bachelor caldera resulted in collapse of blocks near the top of the elongate dome and in longitudinal faulting striking NNW along the axis of the dome (fig. 2). The Amethyst fault, one of four major ore-producing vein systems, closely follows the trend of one of these faults formed during resurgent doming of the Bachelor caldera (Steven and Ratte, 1965) (fig. 3).

Resurgent doming of the Creede caldera, the youngest of the seven calderas in the central San Juan Caldera Complex, was followed by eruption of rhyodacite, quartz latite, and rhyolite lavas of the Fisher Quartz Latite and deposition of the Creede Formation in the structural moat of the caldera. The Fisher Quartz Latite has been dated at 26.4 million years (Lipman et al., 1970). The Creede Formation consists

Table 1. Volcanic Stratigraphy of the Central San Juan Mountains (Modified from Steven and Eaton, 1975)

Lavas and sedimentary rocks	Ash-flow tuffs (caldera sources)	Composition	K-Ar age* (million years)
Hinsdale Formation		Bimodal basalt and rhyolite	>5 <23-25
Fisher Quartz Latite and Creede Formation		Fisher : quartz latite, rhyolite and rhyodacite lavas and breccias Creede : stream, lake and pyroclastic deposits and travertine	26.4
	Snowshoe Mountain Tuff (Creede)	Phenocryst-rich quartz latite	>26.4 < 26.7
	Nelson Mountain Tuff (San Luis)	Phenocryst-rich quartz latite	>26.4 < 26.7
	Rat Creek Tuff (San Luis)	Ranges from poorly welded phenocryst-poor rhyolite to densely welded phenocryst-rich quartz latite	>26.4 < 26.7
Local rhyolitic, quartz latitic, and andesitic flows and breccias between ash-flow units	Wason Park Tuff	Phenocryst-rich rhyolite	>26.4 < 26.7
	Mammoth Mountain Tuff	Ranges from phenocryst-poor rhyolite to phenocryst-rich quartz latite	26.7
	Carpenter Ridge Tuff -Bachelor Mountain Member -Outflow Member (Bachelor)	Phenocryst-poor rhyolite	>26.7 < 27.8
	Fish Canyon Tuff (La Garita)	Phenocryst-rich quartz latite	27.8
Conejos Formation		Andesitic flows and breccias	35-30

*K-Ar ages from Lipman, Steven, and Mehnert (1970).

of talus-regolith, pyroclastic deposits, stream bed and lakebed deposits, and travertine from mineral springs, all deposited in the low-lying structural moat of the Creede caldera. Mineralization in the district fills faults that cut the Fisher Quartz Latite, the Creede Formation, or both (Steven and Ratte, 1965). Adularia deposited along the OH vein during the early stages of mineralization and illite from hydrothermally altered rocks at the top of the system have been dated at 24.6 $\pm$ 0.3 million years (K-Ar) (Bethke et al., 1976). The mineralization occurs at the northern margin of the Creede caldera in the reactivated keystone graben of the Bachelor caldera (figs. 2, 3). The extensional nature of the late faulting in this caldera suggested to Steven and Eaton (1975) that this late period of deformation resulted from intrusion of magma beneath the district, an hypothesis supported by magnetic and gravity data. This postulated intrusion is presumed not only to have caused the distention and faulting, but also to have initiated the hydrothermal events that caused mineralization.

Eruption of the Hinsdale Formation, a bimodal series of basalt-rhyolite lavas, began 25 to 23 million years ago and continued until at least 5 million years ago, covering the entire San Juan volcanic field (Lipman et al., 1970). The postulated pluton, believed to have been responsible for reactivating the keystone graben and possibly initiating the hydrothermal system responsible for the mineralization, may be related to the initial stages of this bimodal basalt-rhyolite volcanism or may be a terminal caldera-related intrusion of Fisher Quartz Latite (Bethke et al., 1976).

The Ag-Pb-Zn-Cu veins at Creede occur as open-space fillings in fractures in devitrified, welded tuffs which show significant, pre-ore, potassium enrichment (Steven and Ratte, 1965). The intra-caldera Bachelor Mountain Member of the Carpenter Ridge Tuff (massive, hard, phenocryst-poor rhyolite) forms the walls of most of the productive veins in the district, although the upper levels of the southern Amethyst and OH veins both cut a paleostream channel filled by coarse, clastic material of the Creede Formation (fig. 3).

HYDROLOGIC SETTING

The hydrothermal circulation system responsible for mineralization was influenced by two major lithologic factors, according to Steven and Eaton (1975). The first is the nature of the Creede Formation sedimentary rocks found along the northern margin of the Creede caldera. Adjacent to the steep outer wall, and in tributary valleys cutting the wall, the Creede Formation consists of very coarse grained, permeable, talus-regolith and interlayered sandstones and conglomerates. However, within the main basin, it consists of fine-grained, relatively impermeable lake and playa deposits and travertine mounds and terraces. This facies distribution is believed to have been a controlling factor in the hydrologic environment that existed during subsequent mineralization. The second important factor is the soft, relatively impermeable, nonwelded to poorly welded tuffs at the top of the Bachelor Mountain Member of the Carpenter Ridge Tuff, which contain no ore. Ascending solutions rose vertically through

open fractures in the welded tuffs until movement was inhibited and largely blocked by the overlying, soft, nearly impermeable tuffs. The solutions then were forced southward where the rhyolite tuffs abut the permeable water-saturated Creede Formation.

Barton et al. (1977, p. 1) described the deposition of ore and gangue minerals according to the following model. "The ores were deposited from a freely convecting hydrothermal system that probably was initially charged by meteoric solutions, although the salts, metals, and sulfur may well have been derived from deeper sources. The circulating solutions deposited gangue and ore minerals near the top of the convecting cell in a hypogene-enrichment process that extracted metals and sulfur from whatever sources were available at depth and swept them toward the surface. Boiling, with loss of acid components (H_2S and CO_2) which recondensed in the cooler, overlying rocks, led to the formation of an intensely altered, sericitic capping above the ore. Precipitation of ore is attributed to cooling and perhaps to a slight pH rise complementary to the loss of acid constituents through boiling."

Bethke and Rye (1979, p. 1832), in their study of the hydrogen and oxygen isotopic signatures of the ore- and gangue-mineral-forming fluids, suggested that "... waters from three coexisting reservoirs fed the vein system alternately and episodically during vein formation ..." Their data suggest that waters depositing carbonate minerals were deep-seated, probably dominantly magmatic in origin, and that the waters depositing sphalerite, illite/chlorite, and quartz were dominantly meteoric. The meteoric source for fluids trapped in inclusions in quartz was different from that for the fluids which deposited sphalerite and illite/chlorite. They proposed (p. 1832) that "... the quartz fluids entered the vein system from reservoirs beneath the mountainous areas to the north in the vicinity of the present Continental Divide, but that the sphalerite and illite/chlorite fluids entered the vein system from a topographically low area to the south along the structural moat of the Creede caldera."

PREVIOUS FLUID-INCLUSION WORK ON SAMPLES FROM CREEDE

Inclusions in samples from Creede have been either the main subject of, or have been used in, at least 23 published studies. These publications are widely scattered and not always easily recognized to contain fluid-inclusion data from Creede samples. Also, some are in volumes of restricted availability, so we summarize the more important results and the significance of each of these items in table 2. Aside from the development of tools and procedures for inclusion study as an integral part of the Creede study, the major results and conclusions that can be drawn from the inclusion studies to date are as follows: 1) The fluids were boiling in the upper levels of the OH vein during at least part of ore deposition. 2) The temperature of the ore fluid ranged (with several oscillations) from ≈200°C to 270°C, and the salinity ranged from ≈5 to 12 wt. % eq. 3) Higher salinity generally accompanied higher temperature, but many exceptions exist. 4) Sudden changes in salinity and temperature with time recorded in zoned crystals of sphalerite correlate exactly with sharp changes in the color zonation. 5) Higher temperatures correlate well, but not perfectly, with higher iron content in the sphalerite.

Table 2. Previous work on fluid inclusions from Creede, and related investigations

Reference	Nature of study	Summary of results and significance[1/]
Barton et al., 1977	Interpretation of all available data up to 1977	Mineral assemblages and fluid-inclusion data used to estimate the environment of ore deposition in terms of temperature, pressure, pH, salinity, Na/K ratio, and total sulfur. These data, combined with evidence on the iron content of sphalerite, are used to propose the probable position (or range) of the environment in terms of a_{S2} and $-a_{O2}$ and a_{S2}-pH space. A possible hydrologic model is proposed based on these data, and its significance to future exploration is discussed.
Bethke et al., 1960	Time-space relationships	(Abstract only) First description of the mineralogy and detailed paragenesis of the Creede ores from the OH vein. Introduction of the concept of sphalerite "stratigraphy" and the benefits to be derived from the use of doubly polished plates of sphalerite. Actual polished plates of sphalerite were projected to illustrate compositional zoning and several stages of alternate precipitation and leaching; this zoning was then used as an index of time in a companion paper by Roedder (1960b) detailing the changes in the fluid composition with time, from a study of fluid inclusions.
Bethke et al., 1973	$\delta^{18}O$, δD, and $\delta^{34}S$ on minerals and fluids	(Abstract only) The δD and $\delta^{18}O$ of surface waters and fluid inclusions in sphalerite, quartz, and hydrous minerals were reported as well as the $\delta^{34}S$ of sulfides and barite. The ore fluids apparently were dominated by late Oligocene meteoric waters enriched in ^{18}O by reaction with rocks. Interpretation of sulfur isotope data remains ambiguous but suggests isotopic and/or chemical disequilibrium in redox reactions involving sulfur.
Bethke & Rye, 1979	Isotopic studies of ore fluids (O, H, C)	Analyses (97) for δD_{H_2O}, $\delta^{18}O_{H_2O}$, or $\delta^{13}C_{CO_2}$ are presented and interpreted in terms of possible sources of the various fluids involved in the several stages of ore deposition. Some δD values were obtained from fluid inclusions in carbonates and quartz, some δD and $\delta^{18}O$ from fluid inclusions in sphalerite, and the rest were estimated from analyses of minerals. Different fluids had different sources and/or wall-rock exchange histories; the carbon was derived from a deep-seated, possibly magmatic source; a substantial meteoric component was present most of the time; two different meteoric waters were involved; caution is needed in use of models involving mixing of magmatic and meteoric waters.
Czamanske et al., 1963	Neutron activation analyses of inclusion fluids for Cu, Mn, and Zn	A sample of white, euhedral quartz crystals, from locality PMB-AA-107 and containing many presumably primary liquid inclusions, plus some vapor inclusions (suggesting boiling) were analyzed. After careful cleaning and then crushing in vacuo (24.5 mg of fluid released), leaching with first H_2O then cold 10% HNO_3 yielded, respectively, Cu, 60 and 150 ppm; Mn, 620 and 330 ppm; and Zn, 410 and 570 ppm. Contamination seems unlikely.

1/ Emphasizing those parts dealing directly or indirectly with fluid inclusions.

Table 2. Previous work on fluid inclusions from Creede, and related investigations (continued)

Reference	Nature of study	Summary of results and significance
Rama et al., 1965	K/Ar "age" on quartz containing inclusions	A 7-g sample of quartz crystal (3-cm diameter) from PMB-AA-107 containing numerous large primary inclusions had no detectable argon. The relatively low concentration of potassium in the inclusion fluid, plus the relatively young age, should result in the accumulation of very little new radiogenic argon since trapping, and unlike some other inclusion fluids, apparently boiling prior to trapping of the inclusions had flushed out all preexisting argon from the inclusion fluid.
Robinson, 1981	Ore mineralogy and fluid inclusions of southern Amethyst vein	Fluid inclusions in quartz from the lower levels have higher Th and salinity than those from the upper levels (235°C -240°C versus 165°C-175°C, and 9-10 versus 5.5-6.5 wt. % equiv., respectively). Some inclusions are reported to have high amounts of CO_2 and/or CH_4 and are presented as indirect evidence of boiling (sic). (The only evidence presented for these gases lies in some measurements of Tm ice "above 0.0°C". Other inclusions showed physical behavior that could be interpreted as metastable superheated ice at high negative pressure, Roedder, 1967) Calculated enthalpy values show a linear relationship with both salinity and elevation, which is interpreted to indicate mixing of fluids.
Roedder, 1960a	Opaque daughter crystals	Several sphalerite samples from a vug at Creede (locations not given) show small opaque daughter crystals, in part triangular in outline (tetrahedra of chalcopyrite ?). Measurements of the volume percent of daughter crystals (and hence the amount of precipitation on cooling) were highly inexact for several reasons, and generally represent maximum values. These ranged from 1 to 100 ppm metal.
Roedder, 1960b	Th, Tm, D/H, crush and leach	(Abstract only) A general decline of salinity and Th from inner to outer zones was found, as well as significant variations in composition and D/H. The inclusions are primary, have not leaked, and provide a possible tool for recognition of epochs of deposition of sphalerite.
Roedder, 1962a	Appearance of freezing runs	Sphalerite from sample ER-57-34 (Tm -3.15°C) was photographed at various temperatures during run; this same sequence of photographs was used in several later publications.
Roedder, 1962b	Appearance of homogenization runs	Same inclusion as that described by Roedder (1962a) is shown at 130, 204.7, 209.8, and 210°C (Th of 210°C).
Roedder, 1963	Tm and Te	Approximately 400 inclusions in sphalerite from ER-57-34 and other localities (and some in quartz and fluorite) showed first melting (Te) of -28.4°C and Tm from -9.4 to -3.3°C, except two large inclusions in quartz with Tm ≈0°C which were presumed to have leaked. A direct correlation of salinity and Th was recognized.

Table 2. Previous work on fluid inclusions from Creede, and related investigations (continued)

Reference	Nature of study	Summary of results and significance
Roedder, 1965a	Movement of bubbles in thermal gradients	(Abstract only) Although not identified therein, the sample of pale yellow sphalerite described and used in the accompanying motion picture sequence was from PMB-AA-107 (cover photograph on Science, v. 140, no. 3565). The bubbles in these inclusions move down the minute thermal gradients established in the sample by casting a shadow over part of the field of view under the microscope.
Roedder, 1965b	Review of Creede study to date	(Abstract only) Roedder reported P. M. Bethke's review (p. 1401) of the concept of "sphalerite stratigraphy" and its connection with inclusion studies, and the economic significance of "disconformities" (i. e., zones of hydrothermal leaching).
Roedder, 1965c	Chemical analyses, Tm and Th, for several zones	The results of vacuum crushing and microanalysis, using the technique of Roedder et al. (1963), are given for inclusions in 10 samples of sphalerite, 6 from the "Dark" zone (i. e., Orange-brown), and 4 from the Outer yellow-white. Average atomic ratios found, relative to Na, were K-0.11; Ca-0.22; Mg-0.027; Cl-1.53; B-0.02; SO_4-<0.02 ("<" unfortunately omitted in typesetting). Most ratios were rather similar for the two zones, but significant differences between these two were found in Cl/Na and Ca/Na; both were appreciably higher in the Outer yellow-white zone. These data, and Th and Tm for ≈400 primary inclusions from the Outer yellow-white, Orange-brown, and Inner yellow-white zones, are given graphically. Includes two photomicrograph plates, in color, of Creede sphalerite.
Roedder, 1970	Crushing stage study of vapor inclusions in quartz	Large primary, apparently empty "steam" or "vapor" inclusions in sample ER-57-25 were found to contain no detectable amounts of noncondensable gases (i. e., $<10^9$ molecules total). The absence of such gases as Ar from fluids that might otherwise be expected to concentrate them suggests that these fluids have boiled and hence been effectively purged of such gases. Other similar samples showed small amounts of noncondensable gases, well under one volume percent.
Roedder, 1972	Primary inclusions of several origins	Photographs of sphalerite from locality PMB-AA-107 and PMB-J-47 used (plate 1) to illustrate primary inclusions, from growth irregularities and "disconformities" (leach zones). Also photographs of ER-57-34 during both heating and freezing runs.
Roedder, 1977	Changes in ore fluid with time	Tm and Th on over 200 primary inclusions from 20 specific subzones in a large sphalerite crystal from locality NJP-X were presented on a plot of Tm versus Th (essentially the same as Figure 11b of the present paper; this same plot was used in another later paper as well). Ten conclusions drawn were that: 1) The variations resulting in the sphalerite stratigraphy are

Table 2. Previous work on fluid inclusions from Creede, and related investigations (continued)

References	Nature of study	Summary of results and significance
Roedder, 1977 (cont'd)		paralleled by changes in the inclusions (this parallelism may indicate but does not require a cause and effect relationship); 2) The fluids did not simply decrease in salinity and temperature with time, as is frequently and implicitly assumed; 3) Even relatively minor changes in sphalerite may correspond to appreciable changes in the ore fluids; 4) The temperature and/or salinity of the ore fluid changed abruptly at each zone boundary but was constant during the deposition of each zone; 5) If such a fine structure is ignored by blind sampling, serious errors can occur in the correlation and interpretation of fluid-inclusion data with the results of chemical analyses of the host and in the assignment of thermal gradients during deposition; 6) Primary inclusions can be recognized adequately in this material; 7) The inclusions have not necked down since they were trapped; 8) The experimental techniques used have excellent precision; 9) No recognizable difference was noted between large (≈450 μm) and small (≈15 μm) inclusions from the same group; and 10) These inclusions obviously did not leak.
Roedder & Andrawes (unpublished)	Gas analyses in Creede inclusions	Crushing in a stream of ultra-pure helium, followed by high-sensitivity gas chromatography, has been applied to selected inclusions in quartz samples from PMB-AA-107 and PMB-AA-109, and sphalerite samples from PBB-35-107, PBB-128-1, PBB-107 and PMB-BS. No gaseous sulfur compounds were detected in any sample. Other than water, only minor CO_2 (≈80 ppm) and traces of (Ar + O_2), N_2, and H_2 were found.
Roedder & Skinner, 1968	Possible leakage of inclusions under external pressure gradients	Inclusions in sphalerite crystals from samples ER-59-48 (sphalerite yellow at 0.5 mm thickness; Th between 200 and 250°C), and ER65-125 (sphalerite greenish yellow-brown at 2 mm thickness; Th estimated at ≈190°C) were examined before and after 166 hours at 2000 bars and 156°C and 144 hours at 4000 bars and 100°C. None leaked at 2000 bars, but 4 out of 17 inclusions leaked at 4000 bars, presumably through visible cracks.
Rosasco & Roedder, 1979	Upper limit on SO_4^{2-} content of ore fluids	Laser-excited Raman spectroscopy, based on back-scattered radiation, was applied to various inclusions in quartz and sphalerite. No evidence for the presence of SO_4^{2-} was found; calibration studies permit placing the SO_4^{2-} concentration certainly at <1000 ppm and probably <500 ppm (0.005 molal) for most ideal (i. e., large and shallow) inclusions in quartz sample PMB-AA-107Q. This is well below the value of 0.02 molal assumed by Barton et al. (1977) for Creede. Inclusions in sphalerite locality ER-57-34 also showed no SO_4^{2-}, but fluorescence of the host sphalerite raised the detection limit to 3000 ppm. Very strong fluorescence of the host prevented measurement of SO_4^{2-} in inclusions in fluorite PMB-BO.

Table 2. Previous work on fluid inclusions from Creede, and related investigations (continued)

Reference	Nature of study	Summary of results and significance
Wetlaufer, P. H., 1978	Consideration of Creede as a fossil geothermal system	Light-stable isotope studies (see Bethke and Rye, 1979) suggest a deep (magmatic?) source for carbonate-depositing solutions and meteoric sources for fluids depositing sphalerite, quartz, adularia, illite, and chlorite, but geochemical studies of the carbonates indicate similar depositional conditions for both carbonate and sulfide assemblages. Fluid inclusions in rhodochrosite (deposited before main ore stage) have Th = 118-250°C and salinities of 9.5 to 10.6 equiv. wt. % NaCl, similar to those of later ore mineral stage. Higher CO_2 pressures may have been the main difference.
Wetlaufer et al., 1979	Consideration of Creede as a fossil geothermal system	Published and unpublished data on fluid inclusions, alteration, isotopic ratios for O and H, and hydrology are summarized to show that Creede is a fossil geothermal system. A large amount of data on δD and $\delta^{18}O$ are given graphically.

6) The fluids present in inclusions in the several stages were chloride solutions with Na>Ca>K>Mg, but the ratios of Na:Ca:Cl in inclusions from two adjacent zones in the D-stage sphalerite differed significantly. 7) The total contents of Cu, Mn, and Zn in the fluid inclusions in one quartz sample were 210, 950, and 980 ppm, respectively. 8) No SO_4^{2-} (i.e., <500 ppm) could be detected in the fluid inclusions in one quartz sample. 9) No sulfur gases, and only very minor CO_2 (≈80 ppm), could be detected in the fluid inclusions from quartz and sphalerite. 10) Isotopic studies of H, O, C, and S show that there were several sources for the materials in the ore fluids, one possibly magmatic and two different meteoric sources.

NATURE AND LIMITATIONS OF THE FLUID-INCLUSION DATA ON Th AND Tm

Data in this report were collected by many workers who used several different heating/freezing stages and documentation procedures; as a result, the data have varying degrees of precision and accuracy. Contributors, other than the authors, include Harvey Belkin, David Forrer, J. Thomas Nash, John Creel, Martha Toulmin, Timothy Muzik, and Pamela Heald-Wetlaufer. Some data were reported only as a range of temperatures of homogenization (in the liquid phase; that is, Th L+V (L), hereinafter termed Th) and/or freezing (that is, the temperature of melting of ice, Tm ice, hereinafter termed Tm) for a designated number of inclusions measured. Many of the fluid inclusions were measured only for either Th or Tm. Many data were obtained before the detailed studies of paragenesis were completed and their position in the "stratigraphic" column (that is, the sequence of growth zones) devised for each mineral is unknown or can be stated only in general terms. For other data, the origin (that is, primary, pseudosecondary, or secondary) of the inclusions is uncertain or unknown. All available data points are listed in Appendices A and B, but not all are plotted in the figures. No interpretation of the secondary fluid-inclusion data has been made, and for this reason, no data known to be from secondary inclusions are plotted on the figures. Data from known or suspected pseudosecondary inclusions are plotted only when they are believed to reflect the conditions at the time of deposition of the mineral zone in which they occur rather than conditions that obtained during a later fracturing or annealing event. The data points plotted are those for which reasonable evidence exists as to inclusion origin and chronologic position. The data in Appendix B from Robinson (1981) are included only to present a complete set of data on fluid inclusions from Creede and are not plotted on any of the figures or discussed extensively in our summary of the quartz data. (Primary, pseudosecondary, and secondary inclusions were not differentiated in Robinson's study.)

Mineral deposition at Creede has been divided into five stages (table 3), and tentative chronologic correlations among the different mineralogies of each vein system have been established (Bethke and Rye, 1979; Wetlaufer, 1977 and 1978). Stages B and D are the periods of major ore deposition at Creede. Except for stage E, all the stages have yielded at least a few fluid-inclusion temperatures although data from the coarse, D-stage mineralization are by far the most abundant. The few data for the earliest A-stage of mineralization come from rhodochrosite and quartz. All data on the early, fine-grained, B-stage sphalerite

Table 3. Summary of the paragenesis of Creede ores (Modified from Bethke and Rye, 1979)

Stage	Characteristics	Distribution
E stage (youngest)	Fibrous pyrite and some marcasite and stibnite; generally high in orebodies and commonly on cross-cutting fractures	District-wide
D stage	Relatively coarse grained sphalerite, galena, chalcopyrite, and quartz, some hematite; silver minerals notably absent; probably stage of illite alteration; subdivided into three substages on basis of color banding in sphalerite; inner yellow-white (IYW), orange brown (OB), and outer yellow-white (OYW)	Northern parts of OH, P, and Amethyst veins; poorly represented on Bulldog Mtn. vein system as developed thus far
C stage	Volumetrically minor, sits on deep etch of earlier B stage; fluorite overgrowing siderite-manganosiderite and quartz; most fluorite subsequently deeply etched --commonly completely removed	Recognized only in northern parts of OH, P, and Amethyst veins thus far
B stage	On OH, P, and northern Amethyst veins, relatively fine grained sphalerite, galena, chalcopyrite, chlorite, hematite, pyrite, and some tetrahedrite-tennantite; on southern Amethyst vein and on Bulldog Mtn., the vein system consists of banded barite-sulfide with quartz; sulfides, mainly sphalerite and galena with much tetrahedrite-tennantite and other sulfo-salts; native silver common	District-wide
A stage (oldest)	Primarily quartz with minor chlorite and sulfide on OH and P veins and on northern 2/3 of Amethyst vein; on southern part of Amethyst vein and on the Bulldog Mtn. vein system, A stage consists mainly of both quartz and rhodochrosite	District-wide

come from sample locality PMB-CC on the OH vein. All available fluid-inclusion data on fluorite are from samples deposited during the C-stage on the OH vein. Most of the fluid-inclusion data on sphalerite and quartz are from the late, coarse D-stage of deposition, although twelve measurements on primary inclusions from A-stage quartz and possibly a few from C-stage quartz have been reported. Most of the data were collected on sphalerite; quartz and fluorite data are less abundant, and only a few barite and rhodochrosite data are available.

Most of the data are for samples from the OH vein (fig. 4), although one set of sphalerite data (locality PMB-KE) as well as the few temperatures on rhodochrosite are from the Bulldog Mountain vein. One of the barite samples is from the Alpha-Corsair vein (fig. 3), and the data on quartz collected by Robinson (1981; Appendix B) are from the Amethyst vein. Within the OH vein (fig. 4), the fluorite samples are from the middle to lower levels of the vein system, beneath the "mixed layer illite-smectite" alteration cap that immediately overlies most of the quartz samples. At present a detailed correlation of stratigraphy and fluid-inclusion temperatures is available only for D-stage sphalerite from three localities: NJP-X, PMB-BS, and PMB-CC; all are located at intermediate levels in the OH vein. Although these sample localities form the basis for a horizontal cross section of the vein, detailed data from higher and lower sample localities will be necessary in order to construct a thermal gradient map for the fluids depositing D-stage minerals throughout the vein.

SUMMARY OF INCLUSION THERMOMETRY

Figure 5 is a plot of all primary and selected pseudosecondary fluid inclusions from the Creede district for which both Th and Tm have been measured, without subdivision by paragenetic stage. Additional inclusions, on which only Th or Tm have been determined, extend the ranges somewhat. Data are available for sphalerite, quartz, fluorite, rhodochrosite, and barite. None of the few data available for barite are plotted because leakage and necking down of barite occurs easily.

All Th data are uncorrected for pressure because fluid inclusions from a number of localities near the top of the deposit demonstrate that the ore fluid was boiling at times, thus, no correction is required, at least for inclusions formed at that time and at those levels. Except during actual boiling, the hydrostatic pressure at the time of trapping of any given inclusion can be delimited but not determined. By definition, it must be greater than the boiling curve, but determination of the amount of this difference requires information on six parameters (Roedder & Bodnar, 1980): 1) sampling depth in the mine; 2) position of the water table above the sample location at the time of deposition; 3) temperature and composition gradients in this hydrostatic column, e.g., due to mixing; 4) effective density decreases in the column from vapor bubbles; 5) deviations from simple hydrostatic head due to constrictions between sample site and water table; and 6) salinity and dissolved gases in the fluid at the time of trapping. The sampling depth in the mine (fig. 4) has a maximum range of 240 meters (at a density of 1.0 = ~ 24 kg/cm^2).

The effect of the second parameter, the position of the water table, is difficult to evaluate. Steven and Eaton (1975), on the basis of geologic reconstructions, placed the water table at ~ 500-800m above the present surface. This would place the maximum hydrostatic depth, for samples from the north end of the lowest level at 1250m (800 + 450; fig. 4), corresponding to a pressure of 125 kg/cm^2 at density = 1.0. However, this value did not necessarily remain fixed throughout ore deposition. If the fluid in the vein above the inclusion is at the point of boiling throughout its length, and the salinity is known, the data of Haas (1971) permit a relatively unambiguous pressure determination, but the probable deviations from this ideal situation (parameters 3-5) make a highly accurate calculation impossible. The amounts of dissolved gases at Creede were probably too small to be of much significance in affecting the vapor pressure of the fluids. The salinity can be determined from Tm and has two effects: it raises the boiling point at any given pressure, and it controls the compressibility of the fluid, i.e., the slope of the isochores. The range of salinities generally found at Creede (~ 5-12 wt. % eq.) results in only a 6°C range of boiling point in the 50-bar pressure range. The slope of the isochores is so high in this temperature range (e.g., 17.5 and 10.8 kg/cm^2/°C for pure water and 10% NaCl respectively at ~ 200°C) that the maximum pressure correction for inclusions at Creede is probably ~ 5°C.

The data plotted in figure 5 shows that Tm for sphalerite ranges from -3.1°C to -8.75°C corresponding to a range of 5.1 to 12.6 wt. % eq.; the Th ranges from 195°C to 274°C, and the data define a generally positive correlation of salinity (negative values of Tm) and homogenization temperature (Th). One group of sphalerite data shown on figure 5 has unusually high salinities for the range of Th, or low Th for the range of salinities (Th=240°C to 255°C, salinity > 10.8 wt. % eq., Tm < -7.25°C). These data are all from locality PMB-KE on the Bulldog Mountain fault system. On the other hand, one aberrant group of inclusions from locality PMB-BS has low salinities (or high Th) relative to the bulk of the data.

All fluorite samples are from the OH-vein system. The samples from the higher levels (ER65-103 and ER65-119) are in the high-Th/low-salinity part of the low-Th group and in the low-Th/high-salinity part of the high-Th group. The data (fig. 5) show two distinct groupings, both of which may occur in the same crystal: one at 213°C to 228°C and -6.5°C to -7.5°C (low-Th group) and a second at 255°C-266.5°C and -6.5°C to -7.5°C (high-Th group). Data points from higher and lower levels within the vein cluster into separate areas within each of these groupings. No detailed paragenetic sequence has been established within the fluorites and hence the time relations between these two groups are not known.

All the rhodochrosite at Creede is from the early, A-stage of mineralization. The three rhodochrosite inclusions for which data are plotted on fig. 5 have Th of 210°C, 218°C, and 230°C and Tm of -7.1°C, -6.2°C, and -6.1°C, respectively. These three measurements are from a single sample locality; thus the data base is much too small to define the relationship of fluids that deposited rhodochrosite to those that deposited the other minerals. However, these data points indicate that fluids forming rhodochrosite are more closely associated in Th/salinity space

with the low-temperature, high-salinity fluids forming some of the much later fluorite that with those forming the D-stage sphalerite, the quartz, or the high-temperature fluorite.

Excluding data by Robinson (1981) there are only eleven fluid inclusions in quartz for which both Th and Tm are known precisely enough to plot (fig. 5), and the data show wide variation. Th is scattered between 215°C and 250°C, and Tm ranges from -3.0°C to -6.65°C. The points plot within the Th/Tm range of fluid inclusions in sphalerite but lack the extremes of Th shown by the sphalerites. The quartz samples of known stage designations for which data are plotted on figure 5 are all from the late D-stage of mineralization.

Figure 6 is a histogram of data on Th of quartz from Creede samples on which A-stage, D-stage, and probable C-stage quartz are differentiated. The twelve measurements of Th on primary inclusions from A-stage quartz range from 192°C to 263°C and average 237°C. The Th range for probable C-stage quartz is 255°C to 276°C. Data on A- and C- stage quartz are too few to define the temperature range of the fluids that deposited A- and C-stage quartz on the OH vein to any degree of certainty.

Robinson (1981) studied fluid inclusions in quartz associated with mineralization that took place early in the paragenesis of Creede ores on the Amethyst vein and probably corresponds to the A-stage (table 3). He found an average Th of 235°C to 240°C and an average salinity of 9-10 wt. % eq. for the lower levels of the mine. The upper levels average 165°C to 175°C and 5.5-6.5 wt. % eq., respectively, for Th and salinity. Values from intermediate levels show a roughly linear relationship to elevation and occur between the values observed for the upper and lower levels. These Th values are in or below the low-temperature end of the range of A-stage quartz temperatures measured on 17 inclusions from one locality (PMB-CA) on the OH vein approximately 2.5km north of the area studied by Robinson. Obviously, insufficient data exist to determine if the same relationship between Th, Tm, and elevation exists on the OH vein as was found by Robinson on the Amethyst vein.

Workers collecting data on fluid inclusions in some D-stage quartz samples from Creede have reported a wide range of Th values from single samples. The tremendous spread of Th for D-stage quartz was collected from presumed primary inclusions, occurring either as isolated fluid inclusions or along growth planes in the crystals. Variations as much as 100°C have been reported from inclusions within a few millimeters of one another. Because these widely varying temperatures do not appear to correlate with different stratigraphic zones in the quartz crystals and because they homogenized at very high temperatures (>280°C), we believe that these samples contain groups of inclusions that initially trapped varying proportions of liquid and vapor from a heterogeneous, two-phase system. Thus, these inclusions cannot be used for geothermometry, which is based on the trapping of a homogeneous phase; however, this indication of trapping of both liquid and vapor in the same inclusion is good evidence that the fluid was boiling at the time of trapping of the fluid inclusions (Roedder, 1979). This assumption is further bolstered by the presence of recognized "empty" or "steam" inclusions in some of these same quartz samples (for

example, Roedder 1970, fig. 7). It is notable that Robinson looked carefully for evidences of boiling in the quartz samples he studied from the southern portion of the Amethyst vein, but found none. The only evidence he presented for boiling lies in some measurements of Tm ice "above 0.0°C". He reports that the physical behavior of some other inclusions could be interpreted as metastable superheated ice at high negative pressure (Roedder, 1967).

Bethke and Rye (1979) reported very small concentrations of noncondensable gases in their crushing of fluid-inclusion samples for isotope analysis. Roedder (1970, fig. 7) and Roedder and Andrawes (unpublished manuscript) found similar evidence for extremely low concentrations of noncondensable gases, but of course, most instances of simultaneous trapping of gas and liquid involve steam and water and do not require the presence of any other gas. As the various processes of formation of ore fluids generally tend to concentrate noncondensable gases in these fluids, their essential absence in inclusions at Creede suggests that such gases have been effectively flushed out, presumably by boiling prior to trapping, and strongly supports the arguments of Barton, et al. (1977) and Steven and Eaton (1975) that the Creede ores were deposited along the top of a freely convecting hydrothermal system.

Values for Th of inclusions in sphalerite from various localities are plotted in figures 7a and 7b. Figure 7a shows the distribution for the samples whose stratigraphy has been established (PMB-BS, PMB-CC, and NJP-X), and figure 7b shows the remaining sphalerite data plotted with all rhodochrosite, quartz, and fluorite data. Samples from PMB-CC contained both the early, fine-grained, B-stage sphalerite and the later, coarse, D-stage sphalerite (measurements on these two stages are plotted separately in figures 7a and 7c). Not enough data are available on the later D-stage sphalerite from PMB-CC to say much about how they correlate with PMB-BS and NJP-X data except to note that the range of values for PMB-CC is approximately the same as that for PMB-BS and NJP-X. The fact that no PMB-CC data are available from the latest substage of D-stage sphalerite deposited accounts for the lack of low temperatures among the data from this locality.

Figure 7a also permits comparison of the range and distribution of values for Th from samples NJP-X and PMB-BS. The NJP-X values reveal a generally trimodal distribution, with an intermediate peak at about 230°C that is not shown by the less abundant PMB-BS data. The absence of this pattern at the PMB-BS locality may be the result of insufficient data. Figure 7a also shows a dissimilarity in the relative number of data points within the two ranges for the two localities. The PMB-BS locality has many more temperatures above 234°C than below, whereas the data on NJP-X are almost equally divided between the two ranges reflecting, perhaps, the higher proportion of outer yellow-white material in the NJP-X samples. The higher temperature data for NJP-X show a strong mode (and mean) at the lower end of the range whereas the PMB-BS temperatures are more uniformly distributed above 234°C. The mode in the high temperature range for both localities occurs at approximately 240-250°C.

Figure 7b shows Th for quartz, fluorite, rhodochrosite, and all sphalerites other than those from the three localities given in figure 7a. The graph shows the separation of the two groups of data on fluor-

ite and the large spread of the data on quartz and rhodochrosite. The data for sphalerite show a similar distribution to those in Figure 7a with a mode around 245°C and a sharp dropoff in abundance above approximately 250-254°C. Th values between 280°C and 300°C for quartz samples probably represent entrapment of mixed liquid-vapor fluids in a boiling system as discussed above.

The salinities of inclusions in sphalerite from PMB-BS, PMB-CC, and NJP-X (fig. 7c) show quite similar distribution patterns and ranges for the three localities. The Tm range from -3.75°C to -6.25°C (6.1-9.5 wt. % eq.) is the most heavily represented for all three localities, with a sharp dropoff in abundance on either side (but particularly the low-salinity side) of these limits. However, the PMB-BS locality has a few more higher salinity inclusions than either NJP-X or PMB-CC. Figure 7d shows all Tm data for quartz, fluorite, and rhodochrosite, as well as for sphalerite from all other localities. The data for sphalerite are spread over a range similar to that seen in figure 7c. The data from rhodochrosite and fluorite are at higher salinities (lower Tm) than most of the quartz values and occur at the high-salinity end of the sphalerite range. Quartz values are spread over a wide range of Tm (-0.65°C to -6.6°C) and are few in number.

FLUID-INCLUSION DATA IN RELATION TO DETAILED STRATIGRAPHIC STUDIES ON SPHALERITE

In addition to the overall paragenetic sequence for the ore stages at Creede, summarized in table 3, from Bethke and Rye (1979), P. B. Barton, Jr., and P. M. Bethke have made extensive, unpublished studies of the detailed "sphalerite stratigraphy" at Creede. These studies were conducted on many doubly polished plates from a series of crystals, as no individual vug appears to have been a site of continuous deposition throughout the history of the deposit. As in any complex stratigraphic correlation, no single criterion is necessarily definitive, hence, Bethke and Barton used a combination of criteria, including transmitted light color and its variability, zones of accidental solid inclusions, birefringence, codeposited minerals, minor-element concentrations, and leached surfaces (that is, disconformities), and, particularly, the sequence of occurrence of such features. Each leached surface represents a time period when the solutions passing a particular point were unsaturated with respect to sphalerite; they may well have been, or become, saturated and deposited sphalerite elsewhere. Vagaries of ore-fluid movement through the tortuous and probably changing channels of rubble in the vein resulted in large differences in the thickness of given zones, and in the relative thicknesses of the various zones, in individual crystals.

Figure 8 illustrates some features of the complex "stratigraphic sequence" that was established for sphalerite from localities NJP-X and PMB-CC, by P. B. Barton, Jr. and P. M. Bethke, and that established by one of us (TLW) for locality PMB-BS, using the same criteria. The correlations between these "stratigraphic sections" (indicated by the heavy lines in figure 8) are based mainly on recognizable sequences of layers from various sphalerite localities, although data from both the

fluid inclusions and the iron content of sphalerite enhance the validity of the correlations. In the D-stage of ore deposition, three major zones of sphalerite stratigraphy can be distinguished in samples throughout the OH vein[1/]: Outer yellow-white (OYW), Orange-brown (OB), and Inner yellow-white (IYW).

These three major zones are divided into subzones (for example, OYW-2 or OB-6) and subdivided again where necessary (for example, OYW-2-1 or OB-6-6). It is important to note that the subzones are simply numbered consecutively from oldest to youngest for each sample and describe the sequence in that sample only. Such numbers cannot be used for correlation between samples. In fact, as a general rule, subzones numbered the same at different localities will not be correlative. This fine subzone structure may be continuous between a number of nearby localities but seldom may be correlated over a large distance within the vein system. For example, either zone OB-4 or OB-2 at locality PMB-CC (fig. 8) may correlate with zone OB-5 at locality PMB-BS, but this zone has no recognized counterpart in NJP-X samples. As a second example, NJP-X samples have no Inner yellow-white zone but have an extremely thick Outer yellow-white zone (approximately one-third of the total thickness). However, PMB-BS and PMB-CC are similar in having narrow Outer yellow-white zones and thick Inner yellow-white zones. Localities PMB-BS and PMB-CC are relatively close together (185 meters, fig. 4) and on the same level at the northern end of the OH vein, whereas NJP-X is 365 meters south of PMB-BS and 30 meters above it in the vein. However, even between PMB-BS and PMB-CC, significant differences exist. For example, at the PMB-CC locality, the lower, lighter colored half of the Inner yellow-white zone (IYW-1 and IYW-2) is thicker and less uniform than that at the PMB-BS locality (IYW-1), and the Orange-brown zone is much narrower.

Data on the correlation between Th, Tm, and the mole percent FeS in sphalerite are available for two localities, PMB-BS and NJP-X. Figures 9a-9d reveal that there is a positive correlation of both Th and salinity (Tm) with mole percent FeS. The electron-microprobe data on the iron content of the sphalerite and the fluid-inclusion data were not collected on the same chips, and hence the thicknesses of the zones studied by the two techniques are not necessarily the same. To plot the points in figures 9a and 9c (PMB-BS), we had to calculate the location of a particular group of fluid inclusions on the basis of its distance from the top of the zone (macroscopically identified by color), compared to the total thickness of the zone. The average temperature of that group of inclusions (or the temperature, itself, where there was only one inclusion) was then plotted against the mole percent of FeS in sphalerite (obtained from the microprobe traverse) corresponding to that same "percent of depth" down in the zone. Figures 9b and 9d (NJP-X), however, were derived by plotting the average temperature for the various subdivisions (for example, OYW-1-1, OYW-1-2, etc.) of a subzone (for example, OYW-1) against the average mole percent FeS in the sphalerite of that zone. Figures 9a-d

---

[1/]These three divisions were called Outer yellow-white, Dark, and Inner yellow-white by Roedder (1965c)

have been plotted with mole percent FeS in sphalerite as a linear function. As this concentration term appears as a logarithmic function on plots of $^{a}S_2$ vs $^{a}O_2$ (Barton et al., 1977), Figures 9a-d could more properly be plotted in terms of log FeS. Such plots of Th or Tm against log FeS remove some of the concave upward curvature, seen in Figure 9b, but otherwise they are topologically similar to plots against mole fraction FeS.

Figure 10 is a plot of all data for primary and selected pseudo-secondary inclusions in D-stage sphalerite of known stratigraphic positions. Data designated "Nash" are from widely separated localities, most of which are in the upper levels of the OH vein (fig. 4), whereas the remaining three symbols indicate data from three specific localities, as shown. The four groups of data points plotted in figure 10 are stratigraphically identified as being from the Outer yellow-white, the Orange-brown, or the Inner yellow-white zones.

These three stratigraphic zones are not equally represented among the four sets of data points for two reasons. First, only a few data have been obtained for the Outer yellow-white and the Orange-brown zones at some sample localities; thus, we have only two PMB-CC and three "Nash" points from the Orange-brown zone. Data points from the Outer yellow-white zone are almost exclusively from the PMB-BS and NJP-X localities, with no PMB-CC points and only one "Nash" measurement. Second, a given zone may be missing at some localities (for example, the Inner yellow-white zone does not occur at the NJP-X locality).

The Outer yellow-white zone is represented by data points within a narrow range of Tm (-3.1°C to -5.05°C; 5.1 to 7.9 wt. % eq.) and a broader range of Th (195°C to 231.5°C). Only one point from the Inner yellow-white zone (with a dubious stratigraphic assignment) occurs within the range of points from the Outer yellow-white zone. With this exception, the solid line A-A' separates all data from the Outer yellow-white zone from those of the other zones. This sharp demarcation suggests that data points falling below this line which come from a zone in sphalerite that is yellow-white, with no other indicator of stratigraphic position, can tentatively be assigned to the Outer yellow-white zone.

Points in the Orange-brown zone have the largest range in Th (213°C to 274°C) and Tm (-3.2 to -8.7°C; 5.2 to 12.5 wt. % eq.) and overlap the more restricted field of the Inner yellow-white zone points.

The data points from the Inner yellow-white zone are spread over a wide range of Th (225°C to 270°C), although their range in Tm is fairly narrow (-4.5°C to -6.7°C; 7.2 to 10.1 wt. % eq.). All but one of the data points from the Inner yellow-white zone fall within a roughly triangular field in figure 10, in which the widest range in Tm corresponds to the lowest values for Th. In this respect, it is very similar to the shape of the field described by the data from the Outer yellow-white zone, but shifted to higher Th and lower Tm (that is, higher salinity). Many of the data points from PMB-BS and PMB-CC from the Inner yellow-white zone are above 240°C whereas most of the points designated "Nash" are below 240°C. The "Nash" data are mainly from localities that are farther south and on higher levels than the PMB-BS or PMB-CC localities (fig. 4).

In figures 11a, 11b, and 11c, the data on inclusions in sphalerite from localities PMB-CC, NJP-X, and PMB-BS, respectively, are plotted in terms of a detailed stratigraphic succession of stages, rather than being grouped into the three main zones. On these three figures, all data points from the oldest sphalerite stage are in the field designated "1," those from the next younger stage are in field "2," and so on. (Note, however, that given field numbers in Figures 11a, 11b, and 11c are not comparable.) Where several fields have the same stage designation, they represent sphalerite of differing ages within the stage. The PMB-CC location provided data from the early, fine-grained, B-stage sphalerite and the Inner yellow-white zone of the D-stage sphalerite, but lacks data from the Outer yellow-white zone and has only two points from the Orange-brown zone. The NJP-X and PMB-BS localities have only D-stage sphalerite, and the NJP-X locality has no Inner yellow-white zone.

The early, fine-grained, B-stage sphalerite of sample PMB-CC (fields 1-9, fig. 11a) yields Th values from 214°C to 241°C (most are <226°C) and salinities of 6.1-10.3 wt. % eq. (Tm -3.8°C to -6.8°C). No trend is apparent, other than oscillation between higher and lower temperatures and salinities. The next younger zone represented is the Inner yellow-white zone (fields 10-14) with Th generally higher than the preceding B-stage sphalerite (229°C to 256°C), and salinities of 7.3 to 9.9 wt. % eq. (Tm -4.6°C to -6.5°C). The last three fields of this period of deposition are marked by higher Th than the first two fields. The two points in the Orange-brown zone (field 15) fall at lower Th than the bulk of the Inner yellow-white zone points. In summary, sample PMB-CC is characterized by oscillating Th and Tm during early, B-stage deposition, an increase in Th at the end of Inner yellow-white zone deposition, and a decrease in Th for the deposition of some portion of the Orange-brown zone.

Figure 11b shows the changes in Th and Tm with time for D-stage sphalerite from the NJP-X locality. Deposition of the Orange-brown zone began at relatively high Th and salinity (field 1, Th 265°C and 9.6 wt. % eq.; Tm -6.25°C), and then both Th and salinity dropped. Th and Tm remained fairly constant for the next period of deposition (fields 2-6, Th 240°C-250°C; Tm -5.25°C to -6.1°C; salinity 8.2-9.4 wt. % eq.), but Th then increased (field 7), and increased again, along with salinity, to field 8. After that, Th and salinities generally decreased (with some oscillation) to the deposition of zone OB-5-1 (field 14), which represents the youngest sphalerite of the Orange-brown zone.

The deposition of zone OYW-1-3, the first segment of the Outer yellow-white zone, began from the coolest and least saline solution found for this locality (field 15, Th 198°C, and salinity 5.1 to 5.7 wt. % eq., (Tm -3.1°C to -3.5°C)). Next the sphalerite-depositing solutions became hotter and more saline (field 16), then decreased slightly in salinity but heated up significantly (fields 17-19) before finally cycling back to finish deposition at a lower Th and slightly lower salinity (field 20). NJP-X deposition is characterized by repeated cycling through different regions of Th-Tm space, with a general decrease of Th and salinity with time. Additional conclusions to be drawn from the NJP-X data are listed in Table 2 (Roedder, 1977).

The changes in the ore-forming fluid recorded in the fluid inclusions at the PMB-BS locality are as oscillatory as those shown by NJP-X and are generally similar to them (fig. 11c). The eleven data points available from the Inner yellow-white zone (fields 1-3) indicate that deposition took place over a narrow salinity range (8.6-10.0 wt. % eq.; Tm -5.5°C to -6.6°C) as the Th increased from 242°C to 270°C. The sequence indicates that salinity increased sharply before deposition of the Orange-brown zone began (field 4) and that the fluid cooled and became less saline (with some oscillation) as Orange-brown zone deposition proceeded (fields 5-9). A relatively constant temperature (236°C-251°C) was maintained for a major portion of zone deposition, excepting one unusual excursion up to higher Th (field 20), although salinity varied widely from 5.4 to 10.1 wt. % eq. (Tm -3.3°C to -6.7°C) during this time (fields 10-21). Salinity and Th decreased during formation of the last part of the Orange-brown zone (fields 22-23), and deposition of the earliest Outer yellow-white zone began with the least saline and coolest fluid evidenced at this locality (field 24), just as was found at the NJP-X locality. Th increased at a relatively constant salinity for the remainder of deposition of the Outer yellow-white zone (fields 25-26).

Several caveats should be mentioned concerning the details of the grouping of data in figures 11a-c into fields by stage. First, from inspection of the small numbers of inclusions defining some of the fields on these plots, it is fairly obvious that the available data probably do not include all oscillations of the ore fluid in Tm-Th space at that particular sampling point. Thus, unless numerous data points define each of a sequential pair of fields, additional smaller scale excursions of the ore fluid are at least possible between these fields. Fields 19-21 in figure 11c provide a good example. All three of these fields are for data from what are believed to be substages in Orange-brown stage 7. Field 20 as drawn encompasses five clustered data points, and one additional much more saline data point at Th = 262.5°C and Tm = -5.8°C. Because the chronologic sequence of trapping of these six inclusions cannot be ascertained, it is impossible to decide between three alternative explanations for this anomalous point: 1) an actual but temporary excursion to more saline fluids during stage 20 growth; 2) a gross misidentification of the host stage for the odd inclusion; or 3) an erroneous Tm measurement. Second, inclusions near a boundary between stages can be misassigned into either adjoining stage as a result of a highly irregular boundary, filling of deep etch pits, etc. (This cannot explain the anomalous inclusion just described). Several examples of such possible misassignment are seen in figure 11b (e.g., field 4) and have been detailed by Roedder (1977).

In summary, deposition of coarse-grained, D-stage sphalerite at these localities apparently began at intermediate salinities (7.8-9.2 wt. % eq.) and intermediate temperatures (approximately 240°C). The data available on the end of Inner yellow-white deposition indicates both increased (PMB-BS, fig. 11c) and decreased (PMB-CC, fig. 11a) temperature and salinity. The dark-colored, iron-rich sphalerite of the early Orange-brown zone was deposited by the hottest, most saline fluids present during D-stage mineralization. The fluid oscillated in both Th and Tm during deposition of the Orange-brown zone, but both values generally decreased. Deposition of the Outer yellow-white zone

began with the coolest, least saline fluids and ended with a trend of increasing temperature at approximately constant salinity.

SPECULATIONS ON THE CAUSES OF OBSERVED Th/Tm VARIATIONS AND THE NATURE OF OUR CONTINUING INVESTIGATIONS

The data from fluid inclusions in sphalerite, the only mineral for which we have currently enough data to make a meaningful interpretation, exhibit a generally positive correlation of salinity (negative values of Tm) and Th, suggesting mixing of hot-saline fluid with cool-fresh fluid. As detailed above, D-stage sphalerite is characterized by repeated cycling through different regions of salinity/Th space, with only a general decrease of Th and salinity with time. At first glance, it would seem that a simple mixing of a hotter, saline and a cooler, fresh water could yield points only along a straight line connecting the two end member fluids on a plot of Tm vs Th such as figures 5, 10, and 11. Deviations from such a straight-line pattern are possible or even likely, however, as shown diagrammatically in figure 12. Let us consider the salinity and temperature of the fluid passing a given point in the vein, a point at which a growing sphalerite crystal with fluid inclusions records the salinity and temperature. Let us also assume no recycling of fluid, in contrast to the mechanism proposed by Barton et al. (1977). If the two end-member fluids are hot-saline and cool-fresh, and a 10-90 mixture of these two has been flowing through the system for a considerable period of time, the fluid passing the given point will be at A and will have salinity S_A, and both it and a large mass of adjacent wall rock will have temperature T_A. Now let the mixing ratio for the fluid entering the vein suddenly be changed to 90-10, equivalent to point B. The cooler type A fluid will be flushed out of the system, causing the salinity of the fluid passing the given point to move toward S_B, and simultaneously, the new, hotter fluid will lose heat to the wall rocks until they are brought up to near T_B. If the effective rock/water ratio at a given moment within the system is high, the fluid passing the given point will approach salinity S_B much more quickly than temperature T_B (i.e., route 1 in figure 12). With lower rock/water ratios, the change in the fluid passing the given point approaches route 2. Conversely, if the sudden change is from fluid B to fluid A, routes 3 or 4 can be followed.

Numerous other processes can also be invoked to explain divergence from a straight mixing line and several may have operated simultaneously. Three possible examples: 1) the end member fluids themselves may vary in salinity or temperature for any of several reasons; 2) changes in the plumbing system may route the fluids (before or after mixing) through wall rocks at a different temperature, yielding a temperature transient; 3) a new route through reactive wall rocks may result in a change in fluid composition, yielding a change in salinity. Superimposed on these real changes in the fluids passing the given point is the possibility of trapping of gas bubbles from incipient boiling or effervescence, yielding a gross (but only apparent) scatter toward higher temperatures (as may have occurred during some quartz crystallization). A rather slight possibility exists for unrecognized necking down, which would disperse the data horizontally away from the mixing line in both directions. Experimental errors must also add to the scatter, but these are smaller by one or two

orders of magnitude than the deviations found.

Although the mechanisms described above may explain some of the scatter shown in figures 5 and 10, the amazing lack of scatter in the data for any given specific zone, and the abrupt changes in the data from one zone to the next, without any tail from one to the other (fig. 11) provide major constraints on the nature of the processes that must have operated, a point previously discussed by Roedder (1977). Thus, the changes in sphalerite color between zones, e.g., from zone 14 to zone 15 in sample NJP-X (fig. 11b), are optically sharp under the microscope (apparently less than a few micrometers), yet the fluids trapped in inclusions in these two zones changed from 242 ± 1°C and 7.5wt. % eq. for 12 inclusions in zone 14 to 198 ± 1°C and 4.3 wt. % eq. for 14 inclusions in zone 15, with no intermediate data points. How can such an abrupt break in the data for successive zones be reconciled with the simple physical requirements of flushing and wall-rock temperature changes illustrated by figure 12? If we assume that fluid flow and sphalerite deposition were both essentially continuous, and that a relatively large volume of fluid flowed through the system during the deposition of each few micrometers of sphalerite, the required chemical and thermal flushing after any abrupt fluid change could be hidden within those few micrometers. Hence, the probabilities of trapping a fluid inclusion of usable size from such intermediate fluids would be slight. The actual times involved are unknown, but would seem to have to be much larger than those suggested by Barton et al. (1977); we are attempting to place some numerical constraints on the time factor via heat flow calculations for specific models. If the deposition was indeed very slow, it simplifies the problem of the growth of the very large perfect crystals of, in part, almost gem quality sphalerite at Creede but exacerbates the problem of explaining how the fluid flow could remain so extremely constant in salinity and temperature throughout the slow deposition of a given zone of uniform sphalerite several millimeters thick.

Knowledge of the direction of flow of the ore-forming fluids throughout the deposit at any given moment would be of great value in understanding the environment of deposition, and possibly in exploration. In theory, if determinations of the pressure at the time of deposition could be obtained for the fluids forming a specific depositional stage throughout the mine, e.g., from the presence or absence of evidence of boiling, the fluid flow paths would be established. However, the relatively small pressures and the numerous factors affecting them, plus the problems of establishing true contemporaneity of the samples, makes such a determination of flow path extremely difficult at best.

Some evidence for mixing of fluids does exist, although Bethke and Rye (1979), in their study of oxygen, hydrogen, and carbon isotopes, decided that little mixing of fluids from different reservoirs took place. Their study of quartz from the Amethyst-vein system included only late, D-stage samples. Robinson (1981) studied quartz samples from early in the paragenesis (probably A-stage) on the southern Amethyst-vein system. He observed a trend of increasing salinity and temperature with depth which he attributed to mixing of a deeper, hotter solution with a cool, shallow one, with the amount of cool fluid decreasing with depth.

Stable-isotope studies of quartz and sphalerite currently underway should help resolve the questions of fluid mixing.

Also, a series of fluid-inclusion studies are underway which will help to define the changing temperature and salinity of fluids that deposited quartz and sphalerite on the OH vein. A detailed look at the variations in Tm and Th of fluid inclusions of different origin in quartz is being undertaken to clarify the quartz stratigraphy and the stable isotopic composition of fluids that deposited different generations of quartz. Preliminary results indicate that fluids in primary D-stage quartz inclusions have thermometric characteristics similar to those in D-stage sphalerite. Nonprimary inclusions have a much lower average salinity but a similar average Th to that found in the primary inclusions. Detailed stratigraphic, fluid-inclusion, and stable-isotope studies of D-stage sphalerite and quartz are also underway to determine the Th/Tm/ isotopic signature of different zones of sphalerite throughout the OH vein. These studies have been undertaken to evaluate the relative importance of mixing of waters from different reservoirs, each with its own temperature, salinity, and isotope signature, as opposed to processes such as boiling, conductive heat loss, and interaction with wall rocks. This evaluation will be based on techniques developed by Fournier et al. (1976) and Fournier (1979) for hot spring waters at Yellowstone and elsewhere.

SUMMARY AND CONCLUSIONS

Fluid-inclusion and isotopic data from the Creede district indicate that the fluid depositing ore and gangue minerals was probably a mixture of at least two fluids and ranged from 185°C to 274°C in temperature and from 1.1 to 13.4 wt. % eq. in salinity. The data from inclusions in sphalerite describe a general trend of decreasing Th and salinity as deposition proceeded, with several reversals. Intermittent boiling of the fluid high in the vein system near the overlying "quartz-mixed layer illite-smectite" alteration cap is indicated by the measurements on D-stage quartz crystals. A-stage quartz shows no evidence of boiling and yields an average Th of 237°C. The few data available on rhodochrosite (very early in the paragenesis) indicate that the fluid that deposited rhodochrosite was more similar to the low-temperature, high-salinity fluids forming part of the much later fluorite than to any of the other fluids. Seventeen data points for sphalerite from one locality (PMB-KE) on the Bulldog Mountain vein suggest a lower temperature for inclusion fluids of a given salinity on the Bulldog Mountain vein than for presumably equivalent fluids on the OH vein, but a detailed stratigraphic correlation has not yet been established.

These studies have also revealed the changing nature of the fluid responsible for sphalerite deposition at different localities in the OH-vein system (figs. 4, 7, 9, 10). Although the conditions of deposition of sphalerite for the localities were generally similar (fig. 9), early stages at NJP-X were more iron rich, and later stages were less iron rich, than presumably equivalent stages at locality PMB-BS. Similarly, during the later, low-temperature portion of Orange-brown zone deposition, although the Th mode was generally very similar (240°C to 250°C), the

salinity at the NJP-X locality was generally higher than that at the PMB-BS locality during the same stage of sphalerite deposition (Tm ≈-5.5°C versus ≈-4.5°C; fig. 10). Most of the Inner yellow-white zone points from the PMB-BS and PMB-CC localities have a higher Th than points from the "Nash" localities, which are mostly farther south and at higher levels in the vein than the PMB-BS and PMB-CC localities (fig. 4, 10). Finally, the highest Th values and salinities make up a greater proportion of the data points from the PMB-BS locality than they do from the NJP-X locality (figs. 7a, 7c). The highest Th and salinities are measured on fluid inclusions trapped in the darkest, most iron-rich sphalerite layers, and these temperature variations must reflect the differing conditions that prevailed at these two localities during similar stages of deposition.

The inclusion data indicate that although the environment of ore deposition changed suddenly and frequently, it was extremely constant during the deposition of a given zone; the inclusion data also suggest that ore deposition may have been a very slow process, of longer duration than that implicit in the model of Barton et al. (1977). Further detailed mineralogical, chemical, thermometric, and isotopic studies currently being undertaken may permit us to trace the Th/Tm evolution of the fluids depositing specific zones of sphalerite as they travelled through the vein system.

References Cited

Barton, P. B., Jr., Bethke, P. M., and Roedder, E., 1977, Environment of ore deposition in the Creede mining district, San Juan Mountains, Colorado: Part III. Progress toward the interpretation of the chemistry of the ore-forming fluid for the OH vein: Econ. Geol., v. 72, p. 1-24.

Barton, P. B., Jr., Bethke, P. M., and Toulmin, M. S., 1971, An attempt to determine the vertical component of flow rate of ore-forming solutions in the OH vein, Creede, Colorado: Soc. Mining Geologists Japan, Spec. Issue 2, p. 132-136 (Proc. IMA-IAGOD Meetings '70, Joint Symp. Vol.)

Bethke, P. M., Barton, P. B., Jr., and Bodine, M. W., Jr., 1960, Time-space relationships of the ores at Creede, Colorado (abs.): Geol. Soc. Amer. Bull, v. 71, p. 1825-26.

Bethke, P. M., Barton, P. B., Jr., Lanphere, M. A., and Steven, T. A., 1976, Environment of ore deposition in the Creede mining district, San Juan Mountains, Colorado: Part II. Age of mineralization: Econ. Geol., v. 71, p. 1006-1011.

Bethke, P. M., Barton, P. B., Jr., and Rye, R. O., 1973, Hydrogen, oxygen, and sulfur isotopic compositions of ore fluids in the Creede district, Mineral County, Colorado (abs.): Econ. Geol., v. 68, p. 1205.

Bethke, P. M., and Rye, R. O., 1979, Environment of ore deposition in the Creede mining district, San Juan Mountains, Colorado: Part IV. Source of fluids from oxygen, hydrogen, and carbon isotope studies: Econ. Geol., v. 74, p. 1832-1851.

Czamanske, G. K., Roedder, E., and Burns, F. C., 1963, Neutron activation analysis of fluid inclusions for copper, manganese, and zinc: Science, v. 140, p. 401-403.

Fournier, R.O., 1979, Geochemical and hydrologic considerations and the use of enthalpy-chloride diagrams in the prediction of underground conditions in hot-spring systems: Jour. Volcan. and Geothermal Research, v. 5, p. 1-16.

Fournier, R.O., White, D.E., and Truesdell, A.H., 1976, Convective heat flow in Yellowstone National Park, in Proc. 2nd U.N. Symposium on the development and use of geothermal resources, San Francisco, 1975: Washington, D. C., U. S. Govt. Printing Office, v. 1, p. 731-739.

Haas, J.L., Jr., 1971, The effect of salinity on the maximum thermal gradient of a hydrothermal system at hydrostatic pressure: Econ. Geol., v. 66, p. 940-946.

Lipman, P. W., Steven, T. A., and Mehnert, H. H., 1970, Volcanic history of the San Juan Mountains, Colorado, as indicated by potassium-

argon dating: Geol. Soc. America Bull., v. 81, p. 2329-2352.

Plouff, C., and Pakiser, L. C., 1972, Gravity study of the San Juan Mountains, Colorado, in Geological Survey Research 1972: U. S. Geol. Survey Prof. Paper 800-B, p. B183-B190.

Rama, S. N. I., Hart, S. R., and Roedder, E., 1965, Excess radiogenic argon in fluid inclusions: Jour. Geophys. Research, v. 70, p. 509-511.

Robinson, R. W., 1981, Ore mineralogy and fluid inclusion study of the southern Amethyst vein system, Creede mining district, Colorado: M. S. thesis, New Mexico Inst. Mining and Tech., Socorro, New Mexico, 85 pp.

Roedder, E., 1960a, Fluid inclusions as samples of the ore-forming fluid: Report of the International Geological Congress XXI Session, Norden, 1960, Part XVI, Genetic Problems of Ores, p. 218-229.

Roedder, E., 1960b, Primary fluid inclusions in sphalerite crystals from the OH vein, Creede, Colorado (abs.): Geol. Soc. America Bull., v. 71, p. 1958.

Roedder, E., 1962a, Studies of fluid inclusions I: Low temperature application of a dual-purpose freezing and heating stage: Econ. Geol., v. 57, p. 1045-1061.

Roedder, E., 1962b, Ancient fluids in crystals: Sci. Amer., v. 207, p. 38-47.

Roedder, E., 1963, Studies of fluid inclusions II: Freezing data and their interpretation: Econ. Geol., v. 58, p. 167-211.

Roedder, E., 1965a, Non-Brownian bubble movement in fluid inclusions - a thermal gradient detector of extreme sensitivity and rapid response (abs.): Geol. Soc. Amer. Spec. Paper 87, Abstracts for 1965, p. 140 (published in 1966).

Roedder, E., 1965b, Report on S. E. G. Symposium on the chemistry of the ore-forming fluids: Econ. Geol., v. 60, p. 1380-1403.

Roedder, E., 1965c, Evidence from fluid inclusions as to the nature of the ore-forming fluids, in Symposium--Problems of postmagmatic ore deposition, Prague, 1963, Volume 2: Prague, Czechoslovakia Geol. Survey, p. 375-384, 13 pls.

Roedder, E., 1967, Metastable superheated ice in liquid-water inclusions under high negative pressure: Science, v. 155, p. 1413-1417.

Roedder, E., 1970, Application of an improved crushing microscope stage to studies of the gases in fluid inclusions: Schweizer. Mineralog. u. Petrog. Mitt., v. 50, pt. 1, p. 41-58.

Roedder, E., 1972, The composition of fluid inclusions: U. S. Geol. Survey Prof. Paper 440, Chapter JJ, 164 p., 12 plates.

Roedder, E., 1977, Changes in ore fluid with time, from fluid inclusion studies at Creede, Colorado, in Proc. Internat. Assoc. Genesis of Ore Deposits, 4th Symposium, Varna, Bulgaria, 1974: Sofia, Bulgaria, IAGOD, v. 2, p. 179-185.

Roedder, E., 1979, Fluid inclusions as samples of ore fluids, Chapter 14 in Barnes, H. L., ed., Geochemistry of hydrothermal ore deposits, 2nd edition: New York, Wiley-Interscience, p. 684-737.

Roedder, E., 1981, Origin of fluid inclusions and changes that occur after trapping, in Hollister, L. S., and Crawford, M. L., eds., Short course in fluid inclusions: Applications to Petrology: Mineralogical Association of Canada, Calgary, May 1981, p. 101-136.

Roedder, E., and Bodnar, R.J., 1980, Geologic pressure determinations from fluid inclusion studies: Ann. Rev. Earth Planet. Sci., v. 8, p. 263-301.

Roedder, E., Ingram, B., and Hall, W. E., 1963, Studies of fluid inclusions III: Extraction and quantitative analysis of inclusions in the milligram range: Econ. Geol., v. 58, p. 353-374.

Roedder, E., and Skinner, B. J., 1968, Experimental evidence that fluid inclusions do not leak: Econ. Geol., v. 63, p. 715-730.

Rosasco, G. J., and Roedder, E., 1979, Application of a new Raman microprobe spectrometer to nondestructive analysis of sulfate and other ions in individual phases in fluid inclusions in minerals: Geochim. Cosmo. Acta., v. 43, p. 1907-1915.

Steven, T. A., and Eaton, G. P., 1975, Environment of ore deposition in the Creede mining district, San Juan Mountains, Colorado: Part I. Geologic, hydrologic, and geophysical setting: Econ. Geol., v. 70, p. 1023-1037.

Steven, T. A., and Lipman, P. W., 1976, Calderas of the San Juan volcanic field, southwestern Colorado: U. S. Geol. Survey Prof. Paper 958, 35p.

Steven, T. A., and Ratte, J. C., 1965, Geology and structural control of ore deposition in the Creede district, San Juan Mountains, Colorado: U. S. Geol. Survey Prof. Paper 487, 90 p.

Wetlaufer, P. H., 1977, Geochemistry and mineralogy of the carbonates of the Creede mining district, Colorado: U. S. Geol. Survey Open-File Rept. 77-706, 134 p., 1 pl., 21 figs.

Wetlaufer, P. H., 1978, Chemical similarities of hydrothermal fluids from diverse sources, Creede Ag-Pb-Zn-Cu district, San Juan Mountains, Colorado (abst.): Geol. Soc. Amer. Abstracts with Programs, v. 10, p. 515.

Wetlaufer, P. H., Bethke, P. M., Barton, P. B., Jr., and Rye, R. O., 1979, The Creede Ag-Pb-Zn-Cu-Au district, central San Juan Mountains, Colorado: A fossil geothermal system: Fifth Symposium of the International Association on the Genesis of Ore Deposits, Snowbird, Utah, August, 1978 v. II, p. 159-164.

Appendix A. - Fluid-inclusion data for barite, fluorite, rhodochrosite, quartz, and sphalerite from Creede, Colorado.

Abbreviations: Workers: DF, David Forrer; ER, Edwin Roedder; HEB, Harvey Belkin; JC, John Creel; JTN, J. Thomas Nash; MT, Martha Toulmin; PHW, Pamela Wetlaufer; TLW, Terri L. Woods; TM, Timothy Muzik; Zone designation: IYW, Inner yellow-white; OB, Orange-brown; OYW, Outer yellow-white; Fluid inclusion origin: P, primary; PS, psuedosecondary; S, secondary; ?, questionable; Color: lt, light; dk, dark; med, medium; org, orange; rd, red; br, brown; yel, yellow; wh, white; Mineral: sph, sphalerite; cpy, chalcopyrite; Temperature modifiers: v., very; sl., slightly; >, greater than; <, less than; +, at least.
Number of fluid inclusions (F.I.): One, except as indicated.
Origin of fluid inclusions: Primary, except as indicated.
Vein system in which inclusion-containing minerals occur: OH vein, except as indicated.
Stage of mineralization in which inclusion-containing minerals occur: Sphalerite and quartz are D-stage, except as indicated. Other minerals, as described on page 15.
Uncertainties in fluid-inclusion measurements: Indicated where known.

Sample #	# of FI	Tm (°C)	±	Th (°C)	±	Zone	Worker	Notes
				Barite				
ER-65-A105		-2.0	0.5				ER	Bulldog Mtn. vein
"		-3.1	0.1				"	" , P?
"	2	-1.8	0.2				"	" , "
PBB-76-31-67		-4.6		105			JTN	Alpha-Corsair vein
				Fluorite				
ER-57-27	2			>242			ER	
"				247	3.0		"	
"				252	1.0		"	
"	?			185	10.0		"	Plane of secondaries
ER-57-27F		-4.0	0.2				JC	
"		-3.8	"				"	
"		-7.3	"				"	
PBB-66-15-67	6	-7.0		213	2.0		HEB	
"	20	-7.0		210-17	"		"	PS
ER-65-103	9	-7.0		219-28	"		"	
"	7	-7.5		221-22	"		"	
"	4	-7.0		226-29	"		"	P?
"	20	-7.5		258-62	"		"	PS?
"	8	-7.0 to -7.5		255-65	"		"	
"	20	-7.5		216	"		"	S?
"	20	-7.0		214	"		"	S?
"	20	4.5		150-68	"		"	S
ER-65-119	4	-6.5	0.2	216	"		"	
"	200	-6.5		214	"		"	
PBB-129-2-60	14	-6.75		258-60	"		"	
"	20			214-17	"		"	S or PS
PMB-BL	4	-6.5		261	"		"	P?
"	16	-7.0		214	"		"	P?
"	20	-4.5		150-68	"		"	S?

Appendix A. - Fluid-inclusion data for barite, fluorite, rhodochrosite, quartz, and sphalerite from Creede, Colorado -- Continued

Sample #	# of FI	Tm (°C)	±	Th (°C)	±	Zone	Worker	Notes
				Fluorite				
PMB-BO	3	-7.0		258-62	2.0		HEB	
PMB-G	10	-7.5		265-68	"		"	
PMB-K	4	-7.5		216	"		"	P?
"	20	-7.5 to -8.5		258-62	"		"	S or PS
				Rhodochrosite				
PMB-UH	2			205			PHW	Sample PMB-UH
"		-6.2		218			"	is from the
"				218			"	Bulldog Mtn. vein
"	2			209			"	
"				215			"	
"				188			"	
"				232			"	
"				238			"	
"				185			"	
"		-6.1		230			"	
"		-7.1		210			"	
"				210			"	
"				189			"	
"	2			199			"	S
"				249			"	

Appendix A. - Fluid-inclusion data for barite, fluorite, rhodochrosite, quartz, and sphalerite from Creede, Colorado -- Continued

Sample #	# of FI	Tm (°C)	±	Th (°C)	±	Zone	Worker	Notes
				Quartz				
ER-57-23b				227	2.0	?	ER	
" -25a		-1.35	0.25			"	"	
" -25b	3	-5.05	0.15			"	"	
" "				223	0.5	"	"	
" "				229	"	"	"	
" "				227	"	"	"	
ER-59-50		<-4.4				"	"	
ER-65-100		-0.5 to -6.9		225-82		"	JTN	
"		-2.7 to -6.3		195-245		"	"	
ER-65-102		-3.3 to -6.6		190-225		"	"	S?
ER-65-103		-3.2 to -5.2		225		"	"	S?
ER-65-115		-6.0		235		"	"	
ER-65-117		-5.2		215		"	"	
ER-65-129		-3.6 to -5.0		190-245		"	"	
ER-65-130		-0.1 to +6.0		190-260		"	"	
ER-65-132		-4.5		225		"	"	
MB-S	4			255-57	4.0	C-stage?	HEB	PS or S
PBB-20-67-59				276	"	"	"	
"				267	"	"	"	
"	4			265	"	"	"	
"	2			268	"	"	"	
"	2			257	"	"	"	PS or S
"	3			255	"	"	"	"
PBB-36-113-59		-4.5 to -5.8		235		?	JTN	", Overlaps lt sph
PBB-44-155-59		-4.9		215		"	"	
"		-4.9		225		"	"	
PMB-AA-107-Qa				190.5	2.0		ER	
" "				232	"		"	
" "				215			"	
" Qd		-2.45	0.05				"	
" "		-2.65	"				"	
" "		-1.15	"				"	
" "		-2.75	"				"	
" "		-4.00	"				"	
" "		-4.35	"				"	
" "		-0.65	0.10				"	
PMB-AA		-6.6	1.0	235			JTN	
PMB-BK				215-30		?	"	
PMB-BY				252.1	0.5		TLW	
"				>395			"	
"				352.6	2.0		"	
"				325.5	"		"	Homogenized to a gas
"				370.0	1.0		"	
"				273.7	0.5		"	
"				369.6	"		"	May be necked down
"				329.2	"		"	
"	3			>400			"	

Appendix A. - Fluid-inclusion data for barite, fluorite, rhodochrosite, quartz, and sphalerite from Creede, Colorado -- Continued

Sample #	# of FI	Tm (°C)	±	Th (°C)	±	Zone	Worker	Notes
				Quartz				
PMB-BY				341-55			TLW	
"				340			"	
"	2			265.5	1.0		"	
"				288			"	
"				260	1.0		"	
"				281	"		"	
"				358	2.0		"	
"				287	"		"	
"				247.5	0.5		"	
"				329	1.0		"	
"				262.5	"		"	
"				327	"		"	
"				305	"		"	
"	2			301	"		"	
"				297	"		"	
"				236	"		"	
"				235	"		"	
"				251.5	"		"	
"				251.4	"		"	
"				302.3	"		"	
"				248.9	"		"	
"				253.1	"		"	
"				246.6	"		"	
"				251.8	"		"	
"				241.8	"		"	
"				298.7	"		"	
"				298.5	"		"	
"				280.2	"		"	
"				247.1	"		"	
"				296.2	"		"	
"	2			237.6	"		"	
"				257.1	"		"	
"				245.0	"		"	
"				316.6	"		"	
"				292.7	"		"	
"				242.3	0.5		"	
"				240.3	"		"	
"				245.2	"		"	
"				249.7	"		"	
"				248.4	"		"	
"				242.8	"		"	
"				238.3	"		"	
"				279.1	"		"	
"				276.6	"		"	
"				217.0	"		"	

Appendix A. - Fluid-inclusion data for barite, fluorite, rhodochrosite, quartz, and sphalerite from Creede, Colorado -- Continued

Sample #	# of FI	Tm (°C)	±	Th (°C)	±	Zone	Worker	Notes
				Quartz				
PMB-BY				310.5	0.5		TLW	
"				233.0	"		"	
"				252.3	"		"	
"				215.5	"		"	
"				233.7	"		"	
"				311.5	"		"	
"				282			"	
"				253.7	0.5		"	
"				256.5	1.0		"	
"				249	"		"	
"				257.5	"		"	
"				278	"		"	May have leaked
"	2			277	"		"	May have leaked
PMB-BZ		-2.8 to -5.9		220-50			JTN	
PMB-CA				196	4.0	A-stage	HEB	
"				247	"	"	"	
"				245	"	"	"	
"				259	"	"	"	
"	3			231	"	"	"	
"				192	"	"	"	
"				263	"	"	"	
"				238	"	"	"	
"	2			257	"	"	"	
"	5			239	"	"	"	PS or S
PMB-J				242	"	A- or C-	"	
"				162	"	stage	"	Leaked ?
"				232	"	"	"	
PMB-X-94				254.4	0.5		TLW	
"				201.1	"		"	
"				235.8	"		"	
"		-3.3		236.8	"		"	
"		-3.0		236.3	"		"	
"				249.4	"		"	
"				243.1	"		"	
"				245	"		"	
"		-5.4		250.3	"		"	
"		-5.4		248.8	"		"	May be necked down
"				272.4	"		"	
"				243.5	"		"	
"				240.6	"		"	
"		-5.7		248.6	"		"	
"				284.2	"		"	
"				238.4	"		"	
"	2			241.5	"		"	
"				239.9	"		"	
"	2			240.4	"		"	
"	2			>300			"	

Appendix A. - Fluid-inclusion dta for barite, fluorite, rhodochrosite, quartz, and sphalerite from Creede, Colorado -- Continued

Sample #	# of FI	Tm (°C)	±	Th (°C)	±	Zone	Worker	Notes
				Quartz				
PMB-X-94				291.8	0.5		TLW	
"				239.5	"		"	
"				236.7	"		"	
"				250.5	"		"	
"				241.1	"		"	
"				233.6	"		"	
"				251.2	"		"	
"				310	"		"	
"				302.3	"		"	
"	3			>330			"	
"		-3.6					"	
"		-3.3					"	
"				242.8	0.5		"	
"				272.6	"		"	
"				288.8	"		"	

Appendix A. - Fluid-inclusion data for barite, fluorite, rhodochrosite, quartz, and sphalerite from Creede, Colorado -- Continued

Sample #	# of FI	Tm (°C)	±	Th (°C)	±	Zone	Worker	Notes
				Sphalerite				
ER-57-28		-4.6 to -4.75		235			MT	Br
"		-3.35					"	All ER-57-28 samples are in lt yel sph (unless otherwise noted)
"		-2.8 to -2.95		225			"	
"		-4.1 to -4.2		197+			"	Br
"		-3.25 to -3.35					"	
"		-3.20					"	
"		-3.35					"	
"		-3.35					"	
"		-3.20					"	
"		-3.25 to -3.35					"	
"				197+			ER	
"				196			"	
"				200	3.0		"	
"	7			197	"		"	
"				218			"	Near br
"				214+			"	"
"	2			216+			"	"
"				214			"	"
"		-4.3 to -4.6					MT	Med br
"		-7.5					"	Dk br
"	6	-2.95 to -3.10					"	Near br
"		-2.8 to -2.85					"	"
"		-3.5					"	"
"		-3.15					"	
"	2	-5.3					"	Br
"	2	-4.5 to -4.6					"	"
"		-4.2					"	Yel br
"		-6.25 to -6.55					ER	All in dark sph
"	11	-5.95 to -6.25					"	"
"	8	-6.25 to -6.55					"	"
"	4	-5.95 to -6.25					"	"
"		-5.95 to -6.25					"	"
"		-6.25 to -6.55					"	"
"	4	-6.25 to -6.55					"	"
"	5	-5.95 to -6.25					"	"
"	4	-6.55 to -7.0					"	"
ER-57-28b		-3.9 to -4.0					"	Pale yel
ER-57-28c		-5.6 to -5.75					"	Yel-br
ER-57-34a				187-202			"	Outer lighter color
"				186-192			"	"
ER-57-34c	3			218	4.0		"	
"	2			223	2.0		"	
"				216	"		"	
ER-57-34j	2	-3.0	0.5				"	Clear yel (outer)
"	4	≈-5.0	"				"	Dk rd-br core
"		≈-5.0	"				"	Med br

Appendix A. - Fluid-inclusion data for barite, fluorite, rhodochrosite, quartz, and sphalerite from Creede, Colorado -- Continued

Sample #	# of FI	Tm (°C)	±	Th (°C)	±	Zone	Worker	Notes
				Sphalerite				
ER-57-34j	5	-5.0	0.5				ER	Med br
ER-57-34k	13	-3.0	"				"	Banded pale yel
ER-59-45C1		-5.75 to -5.8					"	Yel
ER-59-50		-3.0 to -4.0					"	
"		>-4.4					"	
ER-65-103	1	-7.1	0.3	245			JTN	
ER-65-116	1	-4.4	0.1	230	5.0	Inner IYW	JTN	
"	1	-6.4	"	230	"	Outer IYW	"	
ER-65-121	1	-5.2	0.2	240	"	IYW ?	"	
ER-65-127	4	-4.0	0.5	254	2.0		HEB	V. pale yel
ER-65-128	1	-5.9	0.1	220-30	5.0		JTN	
MB-93A	4	-6.8					ER	Dk rd
"-93B	20	-6.6 to -6.7					"	"
" "		-4.3 to -5.0		228	2.0	OYW ?	"	Lt yel surface zone
" "				223	"		"	Yel with br streaks
" "				219	"		"	"
" "				230+			"	"
" "	2			202	2.0		"	"
" "	5			215	"		"	S
"-93C		-3.3 to -3.6					"	Dk rd
" "		≈-7.45					"	"
" "		-7.3 to -7.45					"	"
" "	2	-6.9 to -7.15		264	2.0		"	"
" "		-8.0	0.2				"	Rd-br
"-93D	6	-6.8	"				"	"
" "	5	-6.4 to -6.6					"	Dk rd
"-93E	12	-7.0					"	Dk rd
" "		-6.7	0.2				"	"
"-93F	29	-4.3 to -4.4					"	"
" "	10	-3.3 to -3.6					"	S
"-93G	5	-5.9 to -6.05					"	"
" "		-3.8 to -4.0		230	5.0	OYW ?	"	Lt yel
" "	5			219-30			"	S
"-93Z		-6.8 to -7.1					"	Dk rd
" "		-3.9 to -4.15					"	"
NJP-X	23	-4.8 to -5.0		204.5-207		OYW-1	HEB	
"	4	-4.85 to -4.95		203-203.5		"	"	
"	2	-5.3 to -5.35		213	2.0	Under OYW-1	"	
"	2	-6.1 to -6.15		249	"	"	"	
"	12	-4.65 to -4.85		206	"	OYW-1 ?	"	
"		-4.6	0.05	219	"	OYW-3 ?	"	
"	5	-5.1	"	231	"	Under OYW-1	"	OB-5-2 ?
"	3	-5.5	"	248	"	"	"	OB-5-1 ?
"	4	-5.3 to -5.35		249	"	"	"	"
"		-5.1	0.05	249	2.0	"	"	"
"		-3.7	"	216	"	OYW-4	"	
"		-3.9	"	218	"	"	"	

Appendix A. - Fluid-inclusion data for barite, fluorite, rhodochrosite, quartz, and sphalerite from Creede, Colorado -- Continued

Sample #	# of FI	Tm (°C)	±	Th (°C)	±	Zone	Worker	Notes
				Sphalerite				
NJP-X	2	-4.15 to -4.2		227	2.0	OYW-3	HEB	
"	7	-3.85 to -3.95		224.5-226		OYW-3 ?	"	
"		-4.1	0.05	229	2.0	"	"	1/
"		-5.8				OB-2-5	"	2/
"		-5.9		247		"	"	
"	3	-5.8		248		"	"	
"		-5.8		247		"	"	
"		-5.6		246		"	"	
"		-5.7		247		"	"	
"		-5.7		248		"	"	
"		-5.4		248		"	"	
"		-7.3		258		OB-2-6	"	PS?
"		-7.2		256		"	"	PS?
"		-7.2		257		"	"	
"		-7.2		258		"	"	
"	4	-7.3		256		"	"	
"	2	-6.8				"	"	
"	2	-6.7				"	"	
"	5	-6.8		268		"	"	
"	4	-6.8		269		"	"	
"		-6.1?				"	"	
"		-6.7				"	"	PS?
"		-6.1				OB-2-5	"	
"	3	-6.2				"	"	PS?
"	2	-5.9		262		"	"	
"		-6.1		262		"	"	
"		-6.2		262		"	"	
"	4	-5.4				OB-2-3	"	PS?
"	3	-5.4		241		"	"	
"		-5.4		242		"	"	
"	4	-5.7		248		OB-2-4	"	P?
"	2	-5.6		249		"	"	PS?
"	8	-5.7		248		"	"	
"		-5.7		249		"	"	
"		-5.6				"	"	P?
"	5	-5.6		248		"	"	P?
"		-5.7		249		"	"	"
"		-5.6		249		"	"	P
"		-5.6		248		"	"	"
"		-6.1				"	"	"
"		-5.7		249		"	"	PS?
"	2	-5.7		248		"	"	"

1/ This and all the preceding NJP-X data are not from Roedder (1977) and have not been integrated precisely into the stratigraphy developed for NJP-X. Therefore, they are not plotted on Figure 11b, but are on all other figures which include data for the Th and Tm of sphalerite.

2/ The uncertainties are 0.05°C and 2.0°C for Tm and Th, respectively, unless otherwise noted, for this and the remainder of the NJP-X data on this page.

Appendix A. - Fluid-inclusion data for barite, fluorite, rhodochrosite, quartz, and sphalerite from Creede, Colorado -- Continued

Sample #	# of FI	Tm (°C)	±	Th (°C)	±	Zone	Worker	Notes
				Sphalerite				
NJP-X	2	-5.4		242		OB-2-3	HEB	PS?
"		-5.5		246		"	"	"
"		-5.6		247		"	"	
"		-5.6		247		"	"	PS?
"		-5.6		247		"	"	P?
"	2	-5.6				"	"	"
"	4	-5.3		241		"	"	
"	2	-5.3		242		"	"	
"		-5.5		242		"	"	PS?
"		-5.4		241		"	"	"
"		-5.3		242		"	"	"
"		-5.8		247		OB-1-3	"	
"		-6.2		266		OB-1-2a	"	
"		-6.2		265		"	"	
"	5	-3.9		218		OYW-4	"	PS?
"	3	-3.9		218		"	"	
"	6	-4.0		231		OYW-3	"	
"	7	-4.0		230		"	"	
"	7	-4.0		227		"	"	
"	14	-4.0		228		"	"	Groups of PS
"	5	-4.0		227		"	"	"
"	5	-4.0		226		"	"	
"	4	-4.2		226		"	"	
"	8	-4.6		204		OYW-1	"	Groups of PS
"	3	-4.6		208		"	"	PS
"	20	-3.5		199		OYW-1-3	"	"
"		-3.1		198		"	"	
"	2	-3.3		199		"	"	PS
"	2	-3.2		198		"	"	P?
"		-3.3		199		"	"	
"	3	-4.8		241		OB-5-1	"	P?
"		-4.8		242		"	"	PS
"	2	-4.8		241		"	"	PS?
"		-4.7		242		"	"	PS
"		-4.8		243		"	"	PS?
"		-4.7		242		"	"	"
"	3	-4.8		241		"	"	PS
"		-3.1		198		OYW-1-3	"	P?
"	5	-3.2		199	≈4.0	"	"	PS?
"		-3.2		199		OYW-1-3	"	P?
"	≈15	-3.1		197		"	"	PS
"	2	-6.2		244		OB-4-3	ER	
"	≈50	-5.6				"	"	PS
"		-5.6				"	"	
"		-5.6		242		"	"	PS

Appendix A. - Fluid-inclusion data for barite, fluorite, rhodochrosite, quartz, and sphalerite from Creede, Colorado -- Continued

Sample #	# of FI	Tm (°C)	±	Th (°C)	±	Zone	Worker	Notes
				Sphalerite				
NJP-X		-5.6		242		OB-4-3	ER	
"		-6.1		245		"	"	
"	2	-6.2		246		"	"	
"		-6.6		252		OB-3-3	HEB	P?
"		-6.6		251		"	"	
"		-6.7		252		"	"	
"		-6.3		248		"	"	
"		-6.7		251		"	"	
"		-6.5		251		"	"	
"	2	-6.3		247		OB-4-1	"	
"	5	-6.2		246		"	"	
"	2	-6.2		247		"	"	
"	2	-6.1		246		"	"	
"	2	-6.3		248		"	"	
"		-6.2		248		"	"	
"		-6.2				OB-4-2	"	
"	2	-6.7		251		OB-4-3	"	
"	3	-6.0		244		OB-1-2b	ER	
"	3	-6.0		245		"	"	
"	31	-6.0		244		"	"	PS
"	2	-6.0		243		"	"	"
"		-5.5		244		"	"	
"		-5.5		243		"	"	PS
"	≈80	-6.0		242		"	"	"
PBB-4-17a-59	2	-6.68 to -6.95					"	
" 17b-59	5	-4.3 to -4.6					"	Lt yel-br
" 17-59	5	-4.55 to -4.9					"	Rd
" "	6	-4.55 to -4.80					"	Rd-br
" "	6	-5.5 to -5.75					"	"
" "	4	-4.55 to -4.8					"	"
" "		-3.0 to -3.6					"	"
" "	3	-4.8 to -5.1					"	"
" "	8	-4.55 to -4.8					"	"
" "	5	-5.1 to -5.55					"	
" "	2	-3.4 to -3.7					"	Outer yel
" "	2	-5.3 to -5.6					"	"
" "	5	-2.8 to -3.1					"	"
PBB-10-34-59A	3	-4.8		225	2.0		"	
"		-4.5		214	"		"	Outer yel, near br
"		-4.8					"	
"	≈10	-4.5 to -6		sl.>250	10.0		"	
"	≈100			200-09			"	S or PS
"	≈10			v.sl.>250	10.0		"	S?
"				229	2.0		"	
"				235	"		"	
"				≈250			"	

Appendix A. - Fluid-inclusion data for barite, fluorite, rhodochrosite, quartz, and sphalerite from Creede, Colorado -- Continued

Sample #	# of FI	Tm (°C)	±	Th (°C)	±	Zone	Worker	Notes
				Sphalerite				
PBB-10-34-59A	2			207	2.0		ER	
"	3			237	3.0		"	
"				228-29			"	Med br
PBB-10-35-59	3	-4.4 to -4.5		203	3.0		JC & ER	Inner yel-br
"		"		198	"		"	"
"		"		205	"		"	"
"		"		230	"		"	"
PBB-10-35-59a	5	-3.8	0.2				JC	Outer yel
"	3	-3.8	"				"	Inner br, near wh zone
"	6	-4.1	"				ER	Outer yel
"	4	-4.60	0.05				"	S, "
"	20	≈-9.5	"				"	Pale, yel-wh
"		≈-9.5	"				"	"
"		-6.8 to -7.1					"	Very early wh core
"		-7 to -8					"	
PBB-10-35-59b		-4.65 to -4.9					"	Early yel-wh core
"		-4.9 to -5.2					"	"
"		≈-4.0	0.2				"	Br partly-dk inner zone
"	7	≈-4.0	"				"	Between inner br and outer yel
"	2	-4.2	"				"	Outer yel
"		-3.8	"				"	Org band in outer yel
"		-3.8	"				"	Outer yel
"	2	-4.0	"				"	Org band in outer yel
PBB-10-35b-59	≈19	-4.4 to -4.5		sl.>250			"	Inner yel-wh
"		"		237			"	"
"	2	-3.4					"	Org band in outer yel
PBB-10-35d-59		-4.4 to -4.5		sl.>250	5.0		"	Inner yel-br
"	≈20			sl.>250	"		"	"
"	5	-3.0					"	Outer yel
PBB-10-35d$_3$-59	2	-4.8					"	Inner yel-wh
"		-5.5					"	"
"	≈17	-4.4 to -4.5		240	5.0		"	"
PBB-12-43-59a	8	-3.6 to -4.0		196-98			"	Outer yel
"	4	-5.5	0.2	233-36			"	Uniform yel-br (inner)
"	3	-5.3	"	232-37			"	"
"				≈205	3.0		"	Edge of br-yel
"	3	-4.7 to -5.1		229-34			"	Uniform yel-br near cpy core
PBB-12-43-59a	9	-4.0 to -4.3		197-207			ER	Between yel-br and outer yel
PBB-14-47-59	2	-3.2	0.2				JC	Yel without color
"		-2.8	"				"	bands
"		-4.0	"				ER	"

Appendix A. - Fluid-inclusion data for barite, fluorite, rhodochrosite, quartz, and sphalerite from Creede, Colorado -- Continued

Sample #	# of FI	Tm (°C)	±	Th (°C)	±	Zone	Worker	Notes
				Sphalerite				
PBB-15-51-59a	2	-5.0	0.2				ER	Org, outside outer yel
"	15	≈-5.0	"				"	Outer yel (inside org)
"	9	-3.3	"				"	
PBB-15-51-59A	3	-3.35 to -3.5					"	Yel-br
"	3	-4.9 to -5.45					"	"
"		-2.95 to -3.3					"	"
"	6	-3.5 to -3.7					"	"
"	3	-3.3 to -3.35					"	"
"		-3.7 to -3.9					"	"
" -59b$_1$	12	-4.4	0.2				JC	Yel-wh zone
"	2	-3.1	"				"	"
"		≈-4					"	"
"	2	-4 to -5					"	"
" 59B	≈12	-4.7 to -5.5					ER	S
"		-3.3	0.2				"	Yel-br
"	4	-4.0	0.2				"	"
"		-7.6 to -8.5					"	"
"		-6.7	0.2				"	"
"	3	-3.8	"				"	"
"	3	-3.9	"				"	"
"		-3.1	"				"	"
PBB-24-76-59	4	-5.45 to -5.6					"	
PBB-25-83-59A	2	-5.45 to -6.1					"	Rd zone
"	≈10	-4.5 to -5.0					"	"
" -59B		-5.0 to -5.45					"	"
"		≈-5.45	0.1				"	"
"		-5.45 to -6.1					"	"
PBB-35-107-59	4	-8.15 to -8.5					"	Uniform yel-br
"	6	-7.95 to -8.15					"	"
"	26	-7.6 to -7.95					"	"
"	5	-7.25 to -7.6					"	"
"	3	-6.85 to -7.25					"	"
"	2	-6.35 to -6.85					"	"
"	2	-5.05 to -5.5					"	"
"	2	-4.5 to -5.05					"	"
PBB-44-155-59				240	5.0		JTN	" , dk
PBB-45-161-59	2	≈-6					"	V. pale yel
PBB-59-7-67		-6.7		225	5.0	IYW	"	
PBB-61-9-67		-5.8	0.5	220-35	"		"	
PBB-X		-5.75 to -5.95					ER	Br (interior)
"		-4.8 to -5.1					"	Yel (outer)
"		-3.9 to -4.2					"	"
PMB-AA-107a$_3$	18	-4.7	0.3				"	Multizoned yel-org-br
" a$_4$		≈-6.5	0.5				"	"

Appendix A. - Fluid-inclusion data for barite, fluorite, rhodochrosite, quartz, and sphalerite from Creede, Colorado -- Continued

Sample #	# of FI	Tm (°C)	±	Th (°C)	±	Zone	Worker	Notes
				Sphalerite				
PMB-AA-109s	7	-4.5	0.3				JC	Org and yel (zoned)
"	3	-4.0	"				"	"
"	2	-4.2	"				"	"
"	5	-4.6	"				"	"
"		-4.6 to -5.2					"	Br
"	3	-3.9	0.1				"	Outermost yel
"	3	-4.4	0.2				"	
"		-5.3 to -5.7					"	Lt br zone
"		-4.6 to -4.8					"	Third yel in from
"		-4.4	0.2				"	the outside
PMB-AA		-3.3	0.1	200	5.0	IYW	JTN	
PMB-AI		-5.8	"	238	"	Inner IYW	"	
"		-5.0	"	236	"	Outer IYW	"	S or PS?
"		-3.9	"	195	"		"	
"		-5.2	"	195	"		"	
"		-6.4	"	240	"	Inner IYW	"	
"		-3.8	"	185	"	" "	"	S
"		-3.9	"	195	"		"	PS?
"		-3.8	"	185	"		"	S
PMB-BC		-5.6	"	240	"		"	Dk
"		-3.9	"	195	"	OYW	"	
"		-4.8	"	250-55			"	Dk
PMB-BJ-21765		-4.6	0.2			OB ?	JC & ER	Br core of crystal
"	3	-3.8	"			"	"	"
"		-3.8	"			OYW ?	"	"
"	3	-4.2	"			OB ?	"	"
"	3	-5.2	0.4			"	"	"
"	2	-6.2	0.7			"	"	"
"		-4.6	0.2			OYW ?	"	Yel rim
"	15	-4.6	"			OB ?	"	PS
PMB-BS-X5-1b		-3.8	"	219.5	2.0	OYW-2	TLW	
"		-3.6	"	218.5	"	OYW-1	"	
"		-3.6	"	212.2	"	"	"	
"		-3.7	"	211.6	"	"	"	
"		-4.1	"	208.3	"	"	"	
"		-4.1	"	208.0	"	"	"	
"		-4.0	"	206.4	"	"	"	
"		-3.6	"	203.5	"	"	"	
"		-4.0	"	198.0	"	"	"	PS
"		-4.6	"	184.6	"	"	"	"
"		-3.8	"	201.8	"	"	"	
"				198.4	"	"	"	Melting not detect-
"				195.8	"	"	"	able
"				197.8	"	"	"	"
"		-4.4	0.2	208.6	"	"	"	PS?
"		-4.4	"	201.4	"	"	"	"
"		-3.5	"	202.0	"	"	"	"

Appendix A. - Fluid-inclusion data for barite, fluorite, rhodochrosite, quartz, and sphalerite from Creede, Colorado -- Continued

Sample #	# of FI	Tm (°C)	±	Th (°C)	±	Zone	Worker	Notes
				Sphalerite				
PMB-BS-X5-1b		-5.7		221.5		OYW-1	TLW	PS?, 1/
"		-5.7		216.6		"	"	"
"		-5.8		215.0		"	"	"
"		-5.7		215.0		"	"	"
"		-5.8		209.6		"	"	"
"		-5.8		210.5		"	"	"
"		-5.8		212.0	3.0	"	"	"
"		-5.8		214.5		"	"	"
"		-5.3		227.2		"	"	
"		-5.1		227.5		"	"	
"		-5.0		225.4		"	"	
"		-4.8		225.1		"	"	
"		-5.4		248.3		OB-7	"	
"		-5.5		248.0		"	"	
"		-5.4		247.9		"	"	
"		-5.7		244.3		"	"	
"		-5.4		219.6		"	"	
"		-5.7		241.1		"	"	
"		-6.0		226.6		"	"	
"		-4.9		225.6		"	"	
"		-4.9		222.5		"	"	
"		-4.8		242.6		"	"	
"		-5.0		239.4		"	"	
"		-4.5		246.0		"	"	PS
"		-4.5		243.8		"	"	"
"		-4.5		243.9		"	"	"
"		-4.5		243.1		"	"	"
"		-4.5				"	"	"
"		-4.5		237.4		"	"	"
"		-4.5		239.1		"	"	"
"		-4.6		241.7		"	"	"
"		-4.6		240.6		"	"	"
"				214.0		OYW-1 or -2	"	"
"		-5.6		206.5		OYW-1	"	PS?
"		-5.6		205.5		"	"	"
"				214.5		"	"	"
"		-4.7		177.0		"	"	"
"		-5.8		183.0		"	"	"
"	2	-4.0		242.0		OB-7	"	"
"		-4.0		242.5		"	"	"
"		-4.2		242.0		"	"	"
"		-4.0		241.5		"	"	"
"		-4.0		240.6		"	"	"
"		-4.1		238.7		"	"	"

1/ The uncertainties for Tm and Th are 0.2°C and 2.0°C, respectively, unless otherwise noted, for all data on this page.

Appendix A. - Fluid-inclusion data for barite, fluorite, rhodochrosite, quartz, and sphalerite from Creede, Colorado -- Continued

Sample #	# of FI	Tm (°C)	±	Th (°C)	±	Zone	Worker	Notes
				Sphalerite				
PMB-BS-X5-1b		-3.9		252.0		OB-7	TLW	PS?, 1/
"		-4.1		254.4		"	"	"
"		-4.2		254.4		"	"	"
"		-4.1		253.0		"	"	"
"		-4.3		253.0		"	"	"
"		-4.1		252.9		"	"	"
"		-4.2		252.7		"	"	"
"		-4.1		252.6		"	"	"
"		-5.3		249.8		"	"	
"		-4.7		247.3		"	"	
"		-4.5		244.6		"	"	
"		-4.6		243.6		"	"	
"		-4.2		265.6		OB-7 or -6	"	
"		-3.8		263.5		"	"	
"		-5.8		262.5		"	"	
"		-4.0		257.7		"	"	
"		-3.9		256.0		"	"	
"		-5.7		249.4		OB-7	"	
"				249.7		"	"	
"		-3.9		257.8		"	"	
"		-4.8		247.5		OB-6	"	
"		-4.9		246.5		"	"	
"	2	-4.8		246.5		"	"	
"		-4.9		243.5		"	"	
"		-4.5		248.5		"	"	
"	2	-4.6		247.5		"	"	
"		-3.2		244.5		"	"	
"		-3.4		244.0		"	"	
"		-3.3		242.2		"	"	
"		-3.9		248.4		"	"	
"		-4.2		248.2		"	"	
"		-4.2		247.4		"	"	
"		-4.4		247.2		"	"	
"		-4.9		249.1		"	"	
"		-3.8		250.6		OB-7 or -6	"	
"		-4.0		246.9		"	"	
"		-4.4		246.5		"	"	
"		-4.5		246.3		"	"	
"		-4.4		243.7		"	"	
"				241.6		"	"	
"		-6.4		244.4		OB-7	"	
"		-6.3		243.3		"	"	
"		-6.7		243.2		"	"	
"		-4.3		241.5		OB-6	"	

1/ The uncertainties for Tm and Th are 0.2°C and 2.0°C, respectively, for all data on this page.

Appendix A. - Fluid-inclusion data for barite, fluorite, rhodochrosite, quartz, and sphalerite from Creede, Colorado -- Continued

Sample #	# of FI	Tm (°C)	±	Th (°C)	±	Zone	Worker	Notes
				Sphalerite				
PMB-BS-X5-1b		-4.1		239.1		OB-6	TLW	1/
"		-4.5		241.3		"	"	
"		-4.1		250.4		"	"	
"		-3.7		247.4		"	"	
"		-4.6		246.2		"	"	
"		-5.2		248.6		"	"	
"		-5.2		248.2		"	"	
"				244.5		"	"	
"		-5.2		247.9		"	"	
"		-4.9		247.3		"	"	
"		-5.4		245.7		"	"	
"		-4.6		241.6		OB-5	"	
"		-5.2		248.0		"	"	
"		-5.1		245.3		"	"	
"		-4.5		240.7		"	"	S?
"		-4.5		241.8		"	"	S?
"		-5.9		244.8		"	"	
"		-7.3		257.5		OB-4	"	
"		-7.1		258.4		"	"	
"		-7.7		260.0		"	"	
"		-7.1		258.0		"	"	
"		-8.2		259.7		"	"	
"		-8.2		259.6		"	"	
"		-8.2		259.5		"	"	
"		-8.2		259.2		"	"	
"		-8.2		258.9		"	"	
"		-8.2		260.5		"	"	
"		-7.5		261.1		"	"	
"		-7.0		256.1		"	"	
"		-7.0		255.5		"	"	
"		-7.9		265.9		OB-3	"	
"				265.6		"	"	
"		-7.7		265.5		"	"	
"		-7.6		264.6		"	"	
"				263.5		"	"	
"		-4.0		204.3		OYW-2 or -1	"	
"		-3.9		202.9		"	"	
"		-4.0		204.3		"	"	
"				202.5		"	"	
"		-3.7	0.2	202.5		"	"	
"		-3.4		201.9		"	"	
"				209.0		OYW-1	"	
"				207.7		"	"	
"	2			209.4		"	"	

1/ The uncertainties for Tm and Th are 0.2°C and 2.0°C, respectively, for all data on this page.

Appendix A. - Fluid-inclusion data for barite, fluorite, rhodochrosite, quartz, and sphalerite from Creede, Colorado -- Continued

Sample #	# of FI	Tm (°C)	±	Th (°C)	±	Zone	Worker	Notes
				Sphalerite				
PMB-BS-X5-2a				208.8		OYW-1	TLW	1/
"				234.5		"	"	
"	2			224.9		"	"	
"		-5.1		245.0		OB-6	"	
"		-5.0		246.1		"	"	
"		-5.0		246.4		"	"	
"		-4.7		241.6		OB-5	"	
"		-4.7		238.0		"	"	
"		-5.0		248.6		OB-6	"	
"				245.0		OB-5	"	
"		-4.5		241.3		"	"	
"		-4.3		237.8		"	"	
"		-5.3		235.8		"	"	
"		-7.7		258.0		OB-4	"	
"		-8.1		262.6		"	"	
"		-7.1		267.0	3.0	OB-3 or -2	"	
"		-7.1		263.8		"	"	
PMB-BS-X5-1c		-6.5		263.7		OB-2	"	
"				265.0		"	"	
"		-7.1		263.7		"	"	
"				263.3		"	"	
"		-7.1		262.5		"	"	
"				262.6		"	"	
"		-7.1		262.1		"	"	
"				261.7		"		
"		-7.0				"	"	
"		-6.5		264.8		"	"	
"		-7.2		273.9		OB-1	"	
"		-7.2		272.8		"	"	
"		-7.4		272.7		"	"	
"		-7.2		272.7		"	"	
"		-7.4		272.4		"	"	
"		-7.4		271.9		"	"	
"		-8.6		273.9		"	"	
"		-8.6		273.5		"	"	
"		-5.65		256.5		IYW-2	TLW & TM	
"		-5.7		256.2		"	"	
"		-6.55		269.7		"	"	
"		-6.45		269.3		"	"	
"		-6.45		269.2		"	"	
"		-5.65		260.9		"	TLW "	
"				259.5		"	"	
"		-5.5		259.1		"	"	
"				258.7		"	"	

1/ The uncertainties for Tm and Th are 0.2°C and 2.0°C, respectively, for all data on this page, unless otherwise noted.

Appendix A. - Fluid-inclusion data for barite, fluorite, rhodochrosite, quartz, and sphalerite from Creede, Colorado -- Continued

Sample #	# of FI	Tm (°C)	±	Th (°C)	±	Zone	Worker	Notes
				Sphalerite				
PMB-BS-X5-1c				258.4	2.0	IYW-2	TLW	
"				256.4	"	"	"	
"		-5.6	0.2	255.6	"	"	"	
"		-5.95	"	249.3	"	"	TLW & TM	
"		-6.1	"	246.4	"	"	"	
"		-6.1	"	242.0	"	"	"	
"				257.5	"	"	TLW	
"	3			258.0	"	"	"	
"	2			260.0	"	"	"	
"	3			259.0	"	"	"	
"				257.0	"	"	"	
"				256.0	"	"	"	
"				254.0	"	"	"	
"				253.0	"	"	"	
"				265.0	"	"	"	
"	2			261.0	"	"	"	
"				256.4	"	IYW-2 or -1	"	
"				255.8	"	"	"	
"				255.7	"	"	"	
"				255.3	"	"	"	
"				254.4	"	"	"	
"				254.3	"	"	"	
"	2			258.0	"	IYW-1 ?	"	
"				255.0	"	"	"	
"				257.0	"	"	"	
"				254.0	"	"	"	
PMB-CA		-5.2	0.05	247	"		HEB	
PMB-CC	2	-4.6	0.1			B-stage	DF & HEB	
"		-4.6	"	>205		"	"	
"		-4.6	"	215	3.0	"	"	
"	2	-4.3	"	226	"	"	"	
"		-4.3	"	223	"	"	"	
"		-4.3	"	213	"	"	"	PS?
"		-4.6	"	204	"	"	"	"
"				197	"	"	"	
"		-4.4	0.1	196	"	"	"	PS?
"		-3.6	"			"	"	
"		-4.2	"	218	3.0	"	"	PS
"		-4.2	"	224	"	"	"	
"	2	-5.4	"			"	"	PS
"		-5.4	"	206	3.0	"	"	"
"		-6.1	"			"	"	
"		-5.5	"	253	3.0	IYW-3-4	"	
"	2	-5.5	"	251	"	"	"	
"				252	"	"	"	

Appendix A. - Fluid-inclusion data for barite, fluorite, rhodochrosite, quartz, and sphalerite from Creede, Colorado -- Continued

Sample #	# of FI	Tm (°C)	±	Th (°C)	±	Zone	Worker	Notes
				Sphalerite				
PMB-CC				250	3.0	IYW-3-4	DF & HEB	P?
"	2	-5.4	0.1	252	"	"	"	"
"		-5.4	"	254	"	"	"	"
"		-5.2	"	250	"	"	"	"
"		-4.6	"	214	"	B-stage	"	P?
"		-4.5	"			"	"	PS
"		-5.3	"	221	3.0	"	"	P?
"		-4.7	"	239	"	"	"	"
"		-6.8	"	222	"	"	DF	"
"		-5.4	"	225	"	IYW-1	"	PS
"		-4.3	"			"	DF & HEB	P?
"				230	3.0	"	DF	"
"		-4.6	0.1	237	"	"	"	
"				265	"	IYW-3-1	"	
"		-3.8	0.1	224	"	B-stage	DF & HEB	P?
"		-3.8	"			"	"	PS?
"		-3.8	"	274	3.0	"	"	
"		-4.4	"	217	"	"	"	PS
"		-6.4	"	229	"	IYW-2	"	
"	2	-4.3	"	219	"	"	"	
"		-5.7	"	223	"	B-stage	DF	P?
"				235	"	IYW-3-2	"	
"		-5.7	0.1	253	"	"	"	
"				259	"	OB-3	"	
"		-5.6	0.1	247	"	IYW-3-4	"	
"				232	"	IYW-2	"	
"		-5.7	0.1	254	"	IYW-3-3	"	
"				258	"	OB-1	"	
"		>-6.2	0.1	232	"	IYW-2	"	
"		-5.5	"	255	"	IYW-3-3	"	
"		-4.9	"	241	"	IYW-2	"	
"		-5.5	"	253	"	IYW-3-3	"	
"				258	"	B-stage	"	
"				242	"	OB-5	"	
"				240	"	"	"	
"		-5.1	0.1	215	"	"	"	
"		-5.1	"	227	"	"	"	
"				272	"	OB-1	DF	
"		-6.5	0.1	256	"	IYW-3-2	"	P?
"		-4.5	"	241	"	B-stage	"	"
PMB-J	4			218-19		OYW ?	HEB	Clear sph
PMB-J-47-59A				212-17			ER	Dk rd-br
"	2			208-15		OYW ?	"	Yel-wh
"				267-69			"	Yel-org
"	2			261-70		IYW ?	"	"

Appendix A. - Fluid-inclusion data for barite, fluorite, rhodochrosite, quartz, and sphalerite from Creede, Colorado -- Continued

Sample #	# of FI	Tm (°C)	±	Th (°C)	±	Zone	Worker	Notes
				Sphalerite				
PMB-J-47-59B				269-74		OB ?	ER	Dk rd-br
"	5			240-43		IYW ?	"	Yel-wh
PMB-J-47-A-A	2			230-37		OB ?	"	Dk rd-br
"	3			242-50		"	"	"
"				258-62		"	"	Dk rd-br
"	5			271-75		"	"	"
"				253-67		"	"	Yel under br
"				245-49		IYW ?	"	Yel under yel-br
"				246-48		"	"	Wh core (?)
"				223-36		"	"	"
"	4			210-22		"	"	Wh, sharp etch zone
"	5			251-54		"	"	Yel-wh, deeply etched
"	2			251-55		"	"	Yel zone, next to br
"				236-42		"	"	Wh
"				240-42		"	"	"
"				240-50?		"	"	"
"				204-25+		"	"	"
"	7			240-43			"	
"	2			262-64			"	
"	100			260-65			"	PS
"				244-52		IYW ?	"	
"	3			240-44		"	"	
"	7			259-61		"	"	
PMB-J-47-A-B	19			240-44		"	"	Yel-wh
"	24			248-50		"	"	Wh (core?)
"	2			215-50		"	"	Yel-org
"				249-50		"	"	
"	3			241-45		"	"	Zone inside wh (?)
"				245-48		"	"	Yel-org
PMB-J-47-A-C				270-75		OB	"	Dk rd-br
PMB-J-47A-d	33			242-47		IYW ?	"	Yel-wh
"	3			233-36		"	"	"
"				244-49		"	"	"
PMB-KE-547-71				244			HEB	All PMB-KE samples are
"	2			247	0.2		"	are in org sph unless
"				242	"		"	otherwise noted, and
"		-7.5	0.5	243	"		"	all are from the Bull-
"		-7.5	"	242	"		"	dog Mountain vein.
"		-8.0	"	247	"		"	
"		-7.5	"	247	"		"	
"		-5.25	"	197	"		"	Yel
"		-5.0	"	199	"		"	"
"		-8.0	"	244	"		"	
"		-7.25	"	244	"		"	
"		-8.25	"	244	"		"	
"		-5.0	"	218	"		"	Yel
"		-4.5	"	204	"		"	"

Appendix A. - Fluid-inclusion data for barite, fluorite, rhodochrosite, quartz, and sphalerite from Creede, Colorado -- Continued

Sample #	# of FI	Tm (°C)	±	Th (°C)	±	Zone	Worker	Notes
				Sphalerite				
PMB-KE-547-71		-8.75	0.5	255	0.2		HEB	
"		-6.25	"	252	"		"	
"		-7.9	"	250	"		"	
"		-8.0	"	250	"		"	
"		-5.5	"	205	"		"	Yel
"		-5.0	"	217	"		"	"
PMB-U				240	5.0		JTN	Dk
PMB-X		-4.6	0.1	240	"		"	"
"		-4.9	"	250	"	IYW	"	
"				190-200	"		"	S

Appendix B. - Fluid-inclusion data for quartz from the southern Amethyst vein from Robinson (1981, Table 2).

Sample #	Elevation (meters)	Th (°C)	Salinity (wt. % eq.)
AR16E	2844	175	7.0
"	"	195	7.1
"	"	192	7.5
"	"	194	7.9
"	"	197	9.6
"	"	195	7.1
"	"	202	7.5
"	"	204	9.0
"	"	206	9.4
"	"	209	9.5
"	"	214	6.8
"	"	217	7.2
AR12E	"	219	8.5
"	"	221	6.0
"	"	228	7.6
AR2E	"	222	9.8
"	"	224	7.4
"	"	226	7.8
"	"	225	10.0
"	"	228	10.0
"	"	228	9.8
"	"	234	6.3
"	"	239	6.3
"	"	234	6.4
"	"	239	6.3
"	"	236	6.7
"	"	240	6.8
"	"	231	6.8
"	"	232	7.3
"	"	236	9.7
"	"	237	9.7
"	"	238	9.9
"	"	235	9.8
"	"	234	9.8
"	"	236	9.8
"	"	253	6.7
"	"	250	7.0
"	"	246	9.9
AR1E	"	228	7.2
"	"	228	7.4
"	"	234	5.7
"	"	238	5.7
"	"	237	7.0
"	"	234	7.2
"	"	236	12.9
"	"	238	12.8
"	"	242	12.8
AR20E	"	229	7.8

Appendix B. - Fluid-inclusion data for quartz from the southern Amethyst vein from Robinson (1981, Table 2) -- Continued

Sample #	Elevation (meters)	Th (°C)	Salinity (wt. % eq.)
AR20E	2844	238	8.0
"	"	242	8.1
"	"	243	7.8
"	"	246	7.8
AR13E	"	225	8.0
"	"	230	9.3
"	"	237	9.3
"	"	236	9.5
"	"	244	9.0
"	"	248	9.4
"	"	252	9.0
AR24E	"	222	9.1
"	"	227	9.0
"	"	239	8.5
"	"	241	8.8
"	"	248	9.0
"	"	242	9.2
"	"	252	9.0
"	"	260	8.9
AR4E	"	229	10.0
"	"	239	10.0
"	"	235	10.3
"	"	238	10.6
"	"	243	10.0
AR15E	"	237	8.8
"	"	246	8.6
"	"	250	8.8
AR14D	2880	199	7.4
"	"	232	8.0
"	"	240	9.0
"	"	225	7.5
AR5D	"	191	7.4
"	"	248	10.2
"	"	246	10.2
"	"	227	9.0
"	"	204	9.0
AR13D	"	207	6.5
"	"	215	6.5
"	"	217	6.4
AR11D	"	215	5.7
"	"	178	3.7
"	"	206	5.0
"	"	204	5.2
"	"	219	5.8
"	"	216	4.9
"	"	200	5.0
"	"	215	5.8

Appendix B. - Fluid-inclusion data for quartz from the southern Amethyst vein from Robinson (1981, Table 2) -- Continued

Sample #	Elevation (meters)	Th (°C)	Salinity (wt. % eq.)
AR10D	2880	234	7.0
"	"	223	6.1
"	"	225	6.1
"	"	216	6.1
"	"	220	6.0
"	"	223	6.3
"	"	218	6.4
"	"	228	6.8
"	"	223	6.8
"	"	220	6.0
"	"	228	7.5
"	"	232	7.4
"	"	233	7.4
"	"	230	6.3
"	"	226	6.2
AR1C	2904	168	8.4
"	"	172	9.7
"	"	181	9.6
"	"	182	10.1
"	"	202	9.3
"	"	215	6.6
"	"	213	10.1
"	"	216	10.2
AR2C	"	183	7.4
"	"	181	8.2
"	"	183	7.2
"	"	193	7.7
"	"	199	8.3
"	"	204	8.8
"	"	206	8.2
"	"	203	7.9
"	"	216	8.6
"	"	216	8.9
"	"	221	7.2
"	"	222	9.0
"	"	227	7.2
"	"	235	7.2
"	"	239	7.5
AR3C	"	187	7.4
"	"	189	7.3
"	"	188	6.8
"	"	194	7.9
"	"	195	7.6
"	"	197	7.6
"	"	197	7.4
"	"	197	7.7
"	"	199	7.6
"	"	204	7.5
"	"	205	5.9

Appendix B. - Fluid-inclusion data for quartz from the southern Amethyst vein from Robinson (1981, Table 2) -- Continued

Sample #	Elevation (meters)	Th (°C)	Salinity (wt. % eq.)
AR4C	2904	192	7.4
"	"	192	7.8
"	"	195	7.8
"	"	196	7.9
"	"	200	7.9
"	"	206	7.9
"	"	209	7.8
"	"	207	5.6
"	"	209	6.3
"	"	210	6.8
"	"	212	6.3
"	"	212	5.9
"	"	214	6.1
"	"	213	5.6
CM2-1	3157	153	5.6
"	"	157	5.7
"	"	181	5.8
"	"	183	6.1
"	"	183	5.8
"	"	188	6.8
"	"	192	7.2
"	"	193	6.8
"	"	194	6.3
"	"	201	7.2
CM2-3	"	146	4.3
"	"	151	5.4
"	"	155	5.0
"	"	159	5.4
"	"	164	5.1
CM2-4	"	162	5.5
"	"	164	6.0
"	"	164	5.8
"	"	188	4.2
"	"	179	4.2
CM2-6	"	150	5.1
"	"	153	5.1
CM2-7	"	168	5.4
"	"	174	5.5
"	"	178	7.4
"	"	178	6.0
CM2-16	"	177	5.6
"	"	179	5.4
"	"	183	5.6
CDS4-150	3178	152	3.9
"	"	148	4.6
"	"	152	4.6
"	"	157	4.7
"	"	158	4.9

Appendix B. - Fluid-inclusion data for quartz from the southern Amethyst vein from Robinson (1981, Table 2) -- Continued.

Sample #	Elevation (meters)	Th (°C)	Salinity (wt. % eq.)
CDS4-150	3178	162	4,8
"	"	162	5.0
"	"	155	5.1
"	"	158	5.2
"	"	160	5.6
"	"	158	6.9
"	"	154	5.6
BM71C-360	3185	181	5.4
"	"	184	5.5
"	"	186	5.7
"	"	182	5.8
"	"	191	5.6
"	"	190	5.9
"	"	196	5.9
"	"	185	6.0
"	"	188	6.1

Figure Captions

1. Map of the San Juan volcanic field showing the location of six of the seven calderas in the immediate vicinity of the Creede district. In order of formation they are: (1) LG, La Garita; (2) B, Bachelor; (3) M, Mammoth Mtn; (4) Wason Park (the source area for the Wason Park Tuff was probably marked by a caldera but it is thoroughly obscured by the younger Creede caldera); (5) SL, San Luis; (6) CP, Cochetopa Park; (7) C, Creede. (Modified from Steven and Eaton, 1975)

2. Map showing relation of the Creede mining district to the La Garita, Bachelor, San Luis, and Creede calderas, central San Juan volcanic field, and showing the general distribution of the faulting that resulted from the early extensional events in the Bachelor caldera. The faults shown, however, are only those that were later reactivated and mineralized. (Modified from Steven and Eaton, 1975)

3. Generalized geologic map of the Creede mining district showing the locations of the four major ore-producing vein systems (OH, P, Amethyst, and Bulldog Mountain). Area of map shown in figure 2. (Modified from Steven and Eaton, 1975)

4. Longitudinal section of mine workings along the OH vein (see fig. 3) showing the locations of samples for which fluid-inclusion data are available. The PBB sample localities are designated only with the first number following the "PBB" in the data table (Appendix A), those designated only with one or two letters are PMB samples, and other sample localities are as indicated. The sample localities marked with an (N) are the Nash localities.

5. Graph of Th versus Tm for all primary and selected pseudosecondary fluid inclusions in sphalerite, quartz, fluorite, and rhodochrosite from all studied paragenetic stages at Creede, Colorado. Data points from sphalerite at the PMB-KE locality are differentiated by a circle surrounding the point. Rectangular fields represent groups of fluid-inclusion data that were reported only in terms of ranges for Th and Tm. The numbers in the fields indicate the number of data points included. Numbers beside individual points indicate the number of fluid inclusions having identical values for both Th and Tm. The solid diagonal lines in the upper part of the diagram separate fluorite data points from higher and lower levels of the OH vein. One point for sphalerite at Th = 225°C and Tm = -2.8 to -2.95 falls just out of the figure and has not been plotted.

6. Histogram of Th values for fluid inclusions in quartz. Measurements on nine inclusions that were reported only as being "greater than" a given value are plotted at the minimum temperature given, on the separate, upper baseline.

7a. & 7c. Histograms of Th and Tm, respectively, for primary and selected pseudosecondary fluid inclusions in sphalerite from the three localities for which a stratigraphic column has been worked out (PMB-BS, PMB-CC, NJP-X). B- and D-stage data from the PMB-CC locality are differentiated.

7b. & 7d. Histograms of Th and Tm, respectively, for primary fluid inclusions in quartz, fluorite, rhodochrosite, and all sphalerites other than those from the three localities for which data are plotted in figures 7a and 7c.

8. Stratigraphic columns of representative samples of D-stage sphalerite from localities PMB-CC, PMB-BS, and NJP-X, indicating color variations by the use of varying densities of stippling. The actual color of the sphalerite in plates of several millimeters thickness ranges from dark reddish brown through various shades of orange brown and yellow, to white. The heavy lines correlate the boundaries of the three major zones: Inner yellow-white (IYW), Orange-brown (OB), and Outer yellow-white (OYW). These major zones are divided into subzones (for example OYW-2 or OB-6) and subdivided again where necessary (for example, OYW-2-1 or OB-6-6), all by relative position in the stratigraphic sequence (see text for caveat). In this scheme of zone designation smaller numbers indicate older zones. The dashed line indicates an uncertain correlation. In general, the darker colored areas correspond to zones of higher Fe content (see Barton et al., 1977). The subzones within a given major zone have been given a simple numerical listing from bottom to top, and hence subzones having the same numerical designation (i.e., OB-4 or IYW-2) at different localities do not necessarily correlate.

9a. - 9d. Graphs of Th and Tm versus mole percent FeS in sphalerite from two localities PMB-BS: (9a & 9c; unpublished data from Terri L. Woods), and NJP-X, (9b & 9d; unpublished data from P. M. Bethke). Data from the three main stratigraphic zones: Outer yellow-white (OYW), Orange-brown (OB), and Inner yellow-white (IYW), as well as some subzones within these zones (given in parentheses; see figure 8), are separately indicated. In figures 9b and 9d, subdivisions (for example, OYW-1-1, OYW-1-2, etc.) within the subzones (for example, OYW-1) are graphed separately where data are available but the subzone symbol is used for all the subdivision points.

10. Graph of Th versus Tm for all data points for primary and selected pseudosecondary fluid inclusions in sphalerite from figure 5 that can be assigned to one of the three major stratigraphic zones of D-stage ore deposition: Inner yellow-white (IYW), Orange-brown (OB), or Outer yellow-white (OYW). This includes all points in figure 5 from the Nash, NJP-X, PMB-CC, and PMB-BS localities. Numbers beside individual symbols indicate the number of fluid inclusions having identical values for both Th and Tm. The symbol for each inclusion indicates which of the four sets of data and three zones it represents. Line A-A' separates data on inclusions from the Outer yellow-white zone from data on inclusions in the other two zones.

11a. - 11c. Graphs of Th versus Tm for primary fluid inclusions in sphalerite from three localities on the OH vein. Each numbered field includes all inclusion data from a specific stratigraphic subzone (or pair of subzones), as indicated in the legend (see figure 8). Where numerous fields are indicated for a single subzone they represent inclusions of different ages within the subzone. A detailed stratigraphy for B-stage sphalerite is available only for PMB-CC. Although field #1 always represents the earliest fluid inclusions trapped, and #2 the next subzone, etc., these field numbers are not comparable in 11a, b, and c. "Incs" indicates the number of inclusions measured whose plotted points fall in that field. The total number of data points on each graph is 31, 221, and 126, for PMB-CC, NJP-X, and PMB-BS, respectively. (Note: Only the NJP-X data from Roedder (1977) are included in figure 11b and in the discussion in the text because the other NJP-X data have not been integrated precisely into the detailed chronologic sequence derived for the Roedder (1977) data. All PMB-CC and PMB-BS points from figure 5 are included in figures 11a and 11c.) The odd extension of field 20 on figure 11c is discussed in the text.

12. Schematic representation of the changes expected in mixed fluids passing a given point in the vein after a sudden change in the mixing ratio (see text).

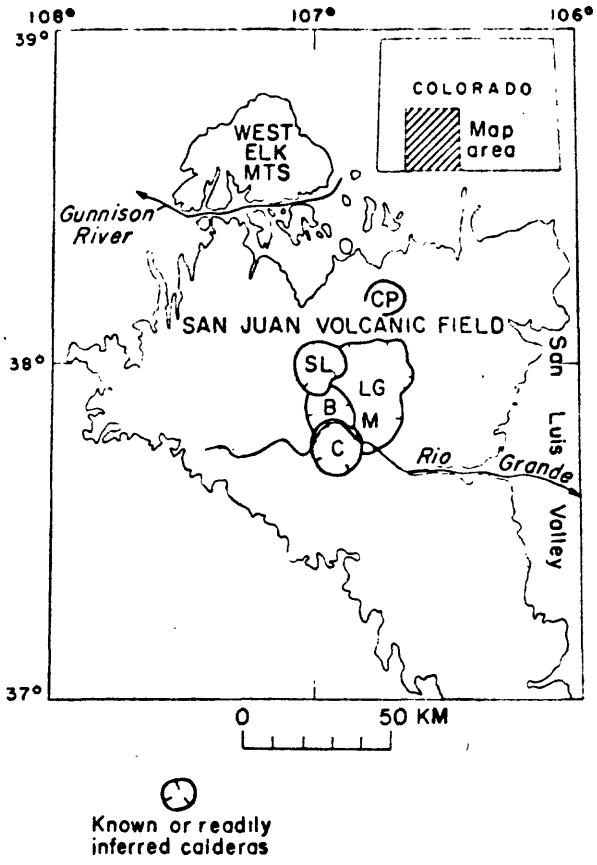
108°
107°
106°
39°
38°
37°
COLORADO
Map area
WEST ELK MTS
Gunnison River
CP
SAN JUAN VOLCANIC FIELD
SL
LG
B
M
C
Rio Grande
San Luis Valley
0
50 KM
Known or readily inferred calderas

Fig. 1

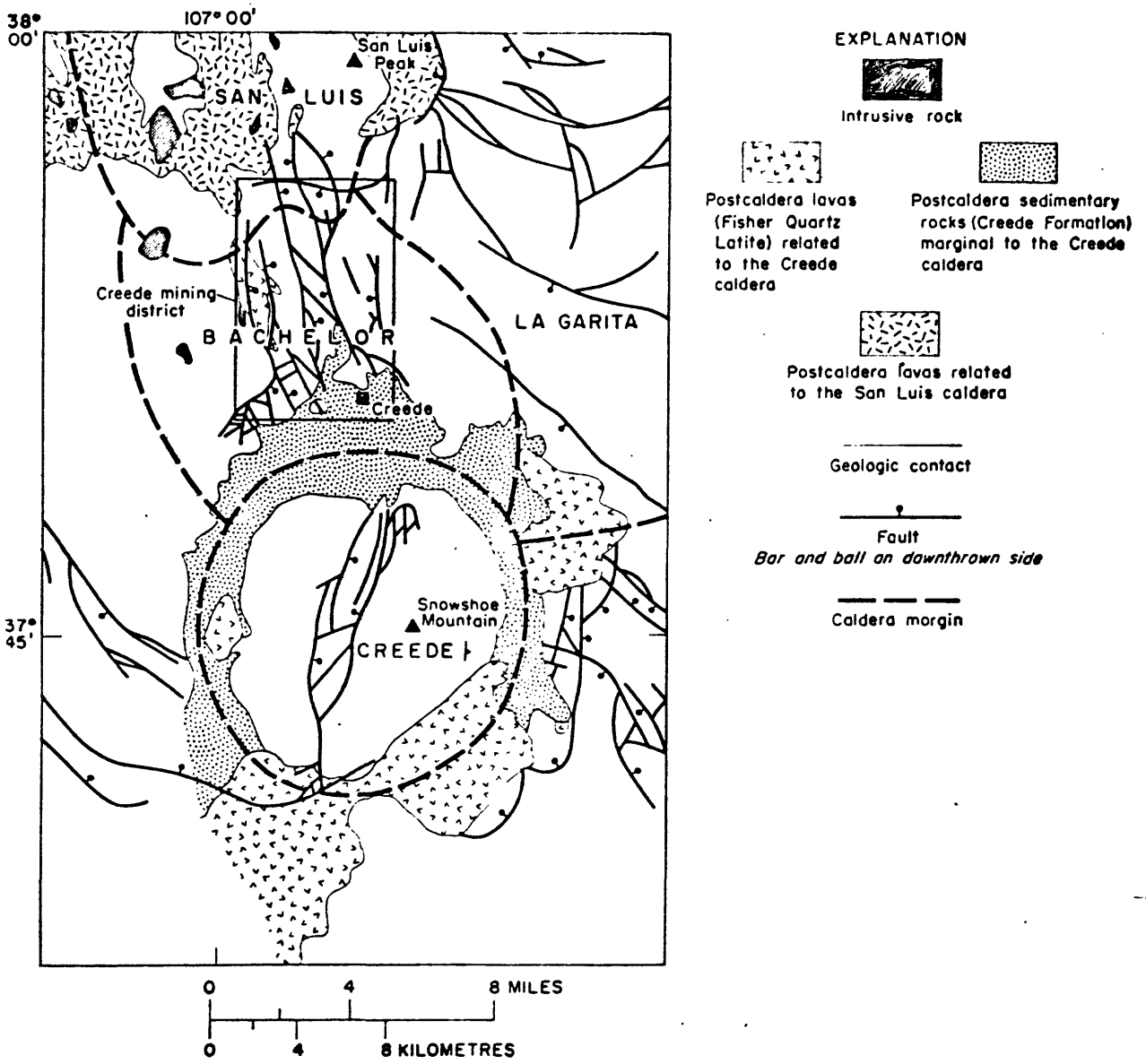
38° 00'
107° 00'
San Luis Peak
SAN LUIS
Creede mining district
BACHELOR
LA GARITA
Creede
Snowshoe Mountain
CREEDE
37° 45'
0 4 8 MILES
0 4 8 KILOMETRES
EXPLANATION
Intrusive rock
Postcaldera lavas (Fisher Quartz Latite) related to the Creede caldera
Postcaldera sedimentary rocks (Creede Formation) marginal to the Creede caldera
Postcaldera lavas related to the San Luis caldera
Geologic contact
Fault
Bar and ball on downthrown side
Caldera margin

Fig. 2

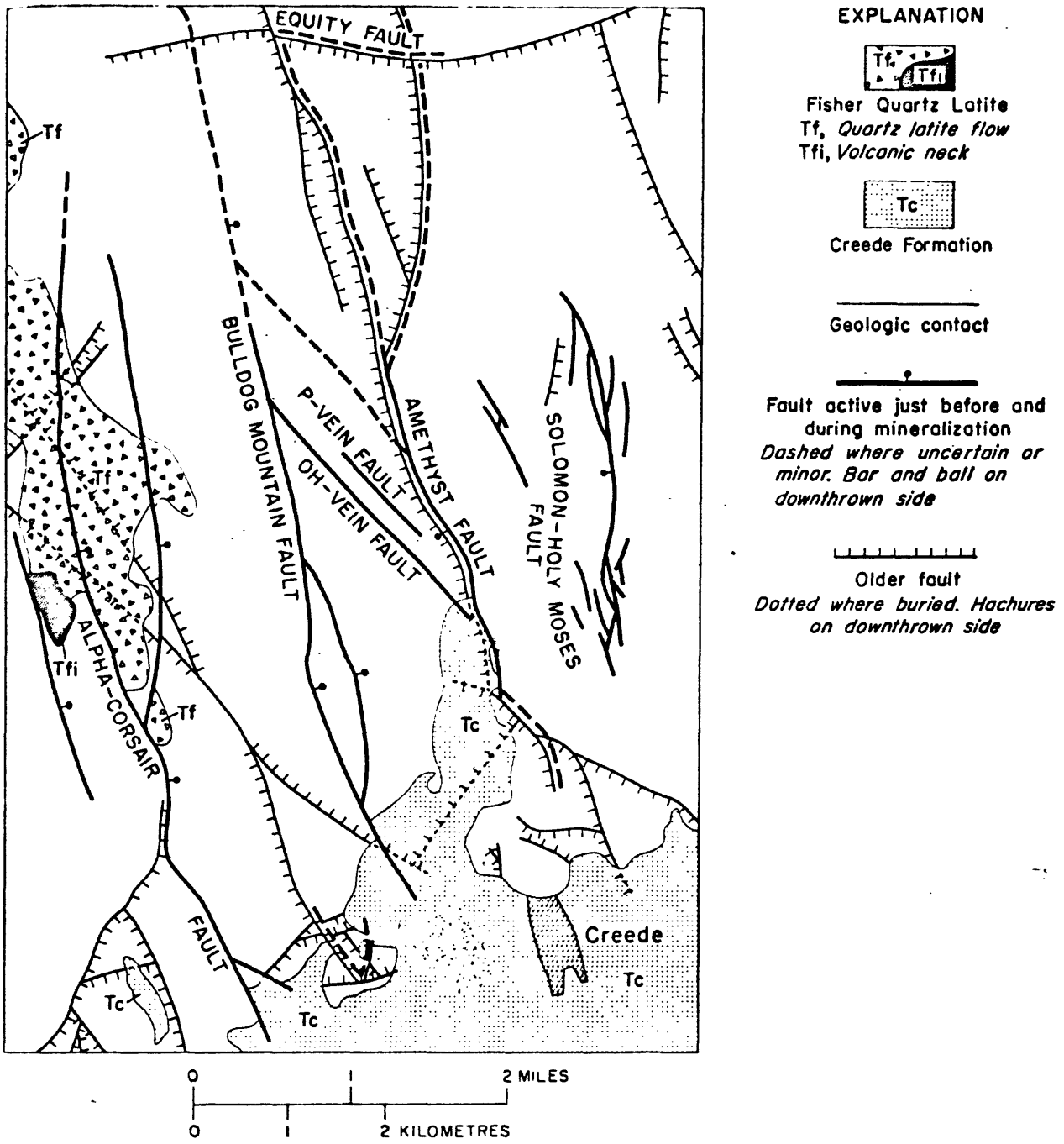
EQUITY FAULT
Tf
Tf
Tfi
Tf
Tc
Tc
Tc
Tc
Creede
Tc
BULLDOG MOUNTAIN FAULT
P-VEIN FAULT
OH-VEIN FAULT
AMETHYST FAULT
SOLOMON-HOLY MOSES FAULT
ALPHA-CORSAIR
FAULT
0 1 2 MILES
0 1 2 KILOMETRES
EXPLANATION
Tf
Tfi
Fisher Quartz Latite
Tf, Quartz latite flow
Tfi, Volcanic neck
Tc
Creede Formation
Geologic contact
Fault active just before and during mineralization
Dashed where uncertain or minor. Bar and ball on downthrown side
Older fault
Dotted where buried. Hachures on downthrown side

Fig. 3

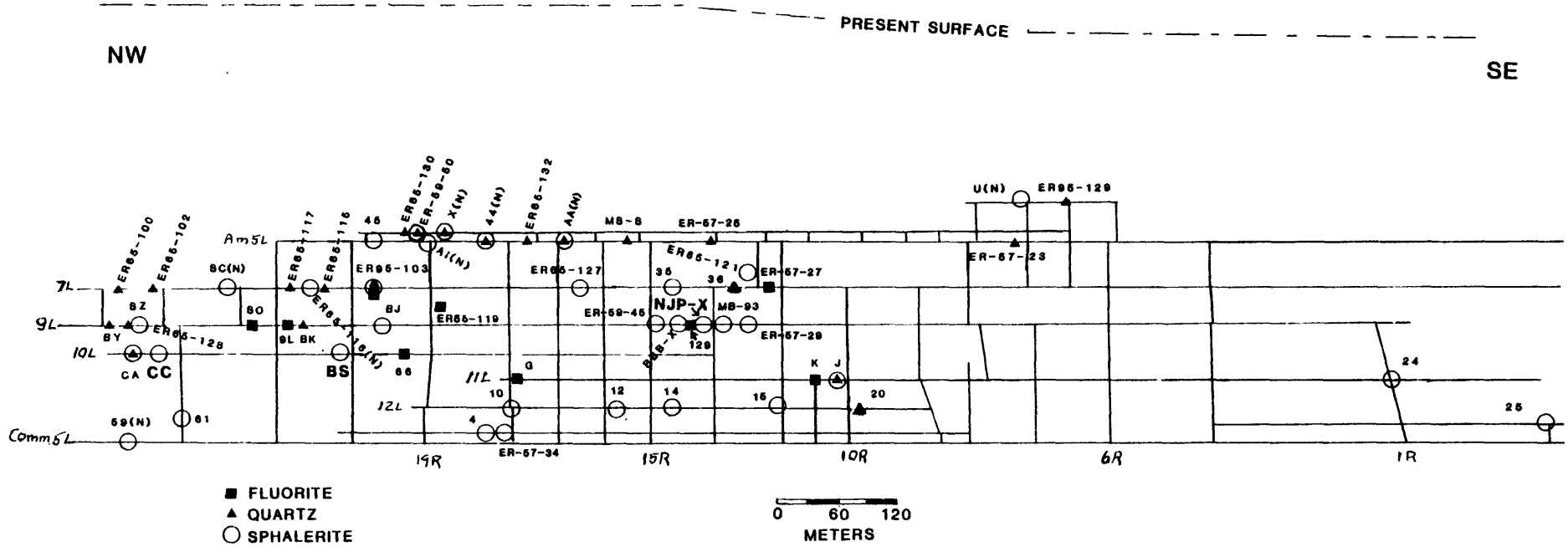
PRESENT SURFACE
NW
SE
ER85-100
ER85-102
Am5L
ER85-117
ER85-116
45
ER85-130
ER-85-80
X(N)
44(N)
ER85-132
AA(N)
MB-8
ER-67-25
U(N)
ER85-129
ER-67-23
7L
SC(N)
ER85-103
AI(N)
ER85-127
ER85-121
35
36
ER-67-27
9L
8Z
8O
BJ
ER85-119
ER-59-45
NJP-X
MB-93
BY
ER85-128
9L BK
ER85-118(N)
129
ER-67-29
10L
CA CC
BS
66
11L
G
K
J
24
10
12
14
15
20
25
12L
4
59(N)
61
Comm5L
19R
ER-67-34
15R
10R
6R
1R
FLUORITE
QUARTZ
SPHALERITE
0
60
120
METERS

Figure 4

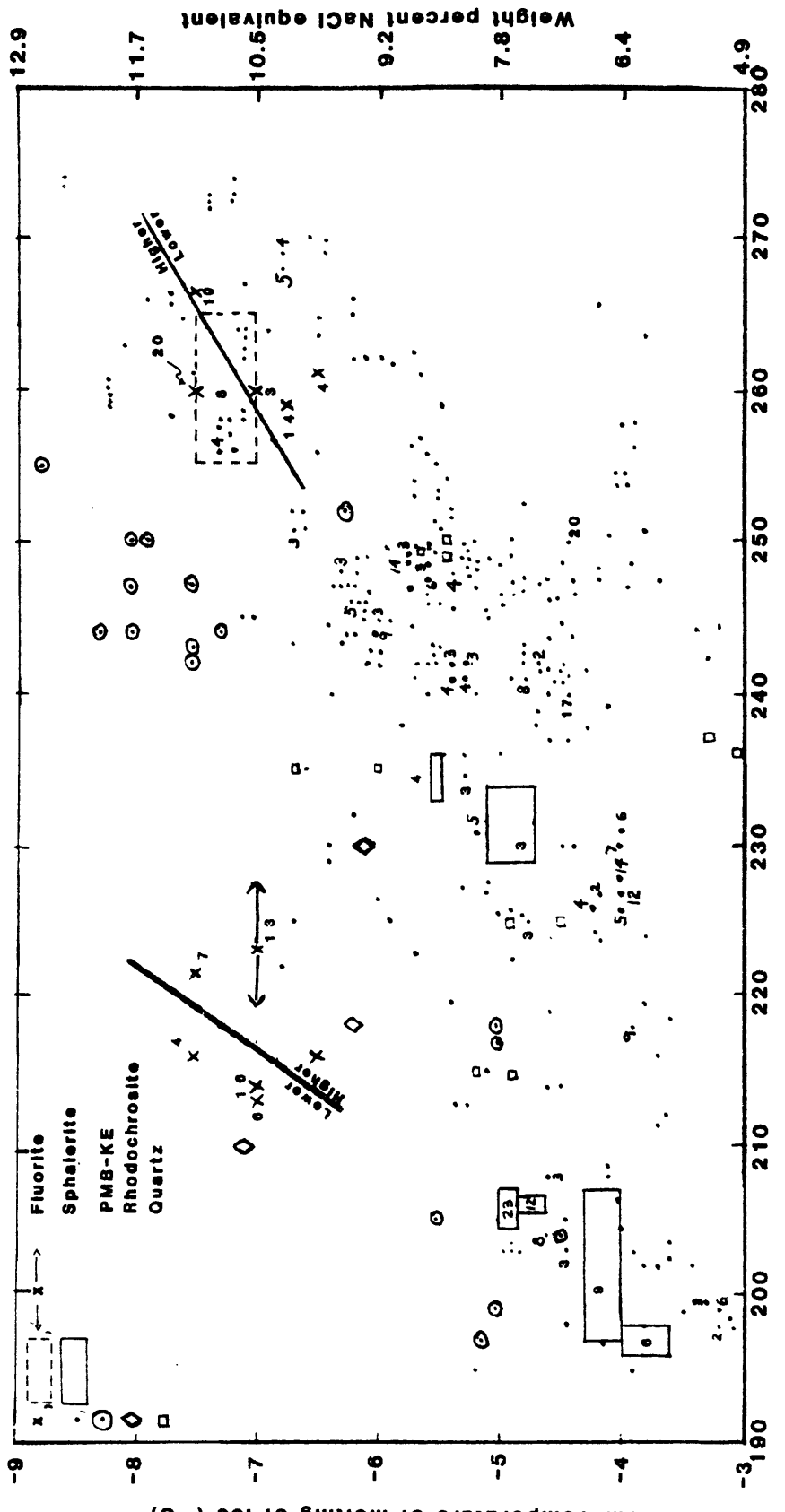
Weight percent NaCl equivalent
12.9
11.7
10.5
9.2
7.8
6.4
4.9
Tm-Temperature of melting of ice (° C)
-9
-8
-7
-6
-5
-4
-3
Th-Homogenization temperature (° C)
190
200
210
220
230
240
250
260
270
280
Fluorite
Sphalerite
PMB-KE
Rhodochrosite
Quartz
Higher
Lower

Figure 5

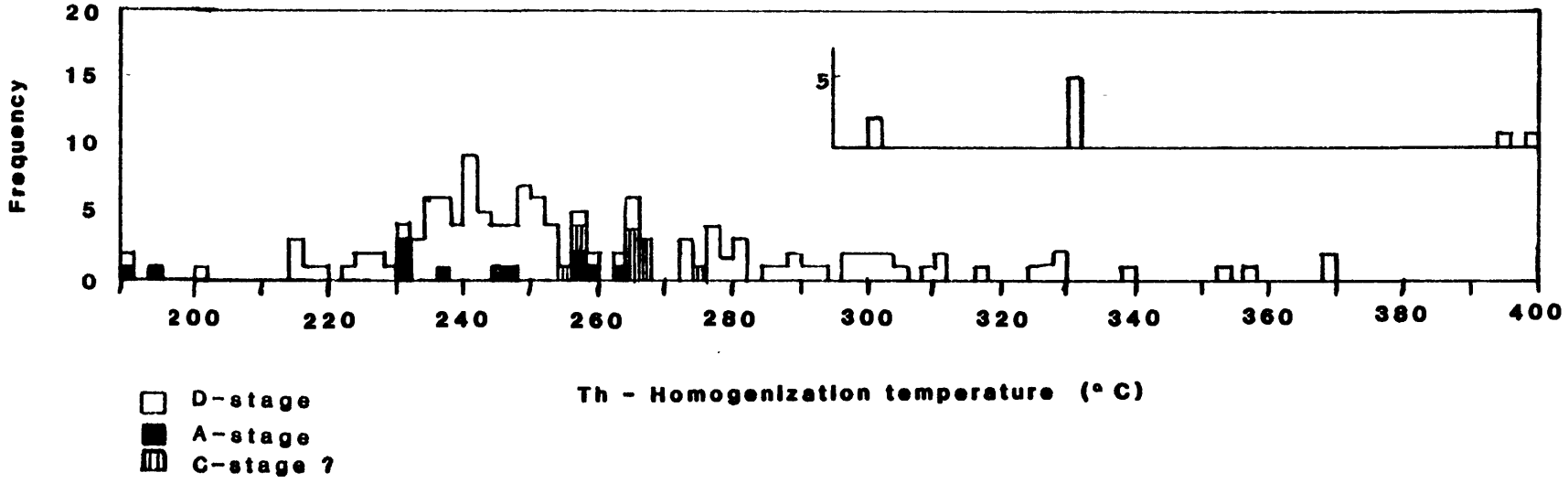
20
15
10
5
0
Frequency
5
200
220
240
260
280
300
320
340
360
380
400
Th - Homogenization temperature (° C)
D-stage
A-stage
C-stage ?

Figure 6

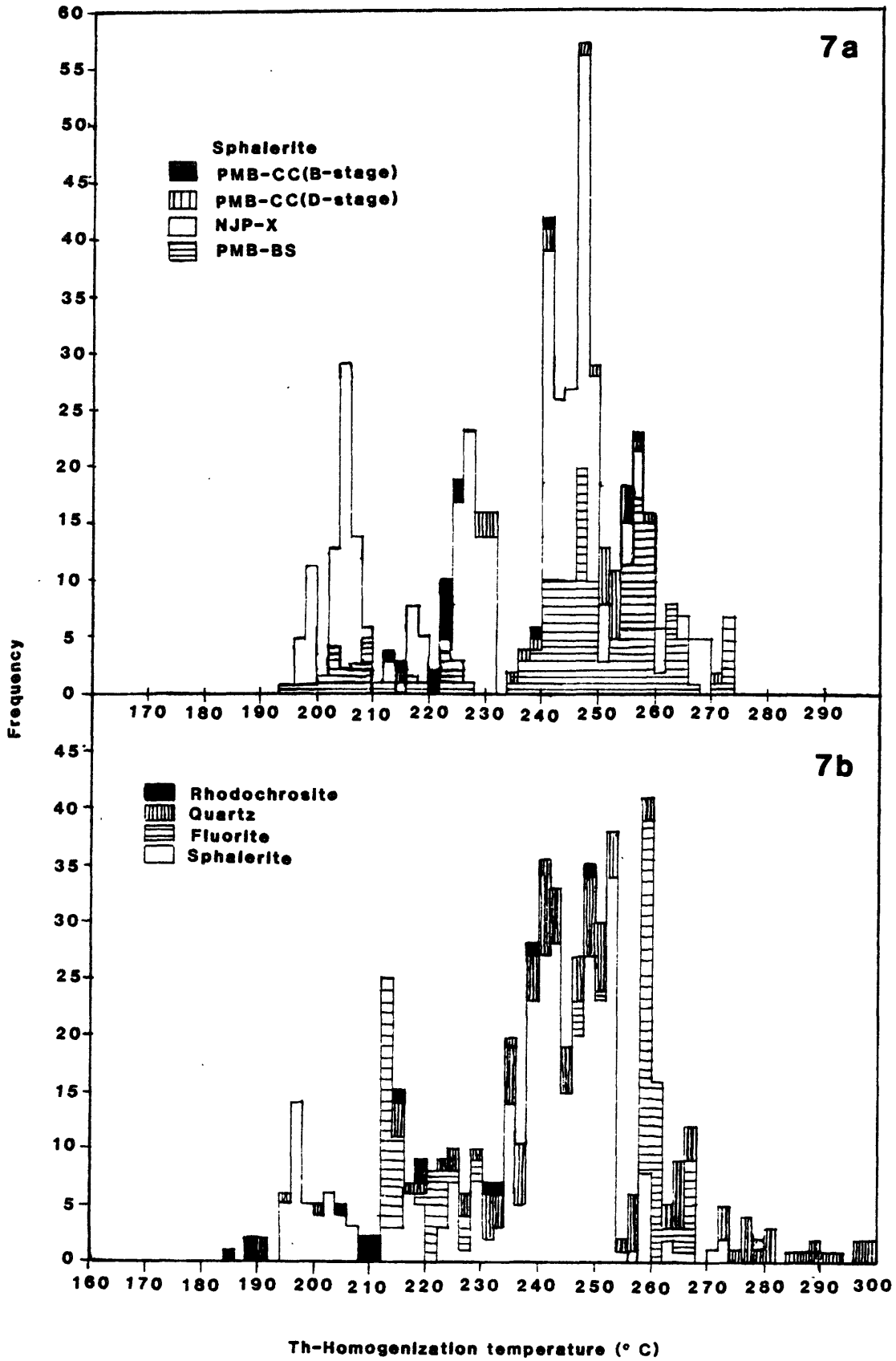
7a
Sphalerite
PMB-CC(B-stage)
PMB-CC(D-stage)
NJP-X
PMB-BS
Frequency
7b
Rhodochrosite
Quartz
Fluorite
Sphalerite
Th-Homogenization temperature (° C)

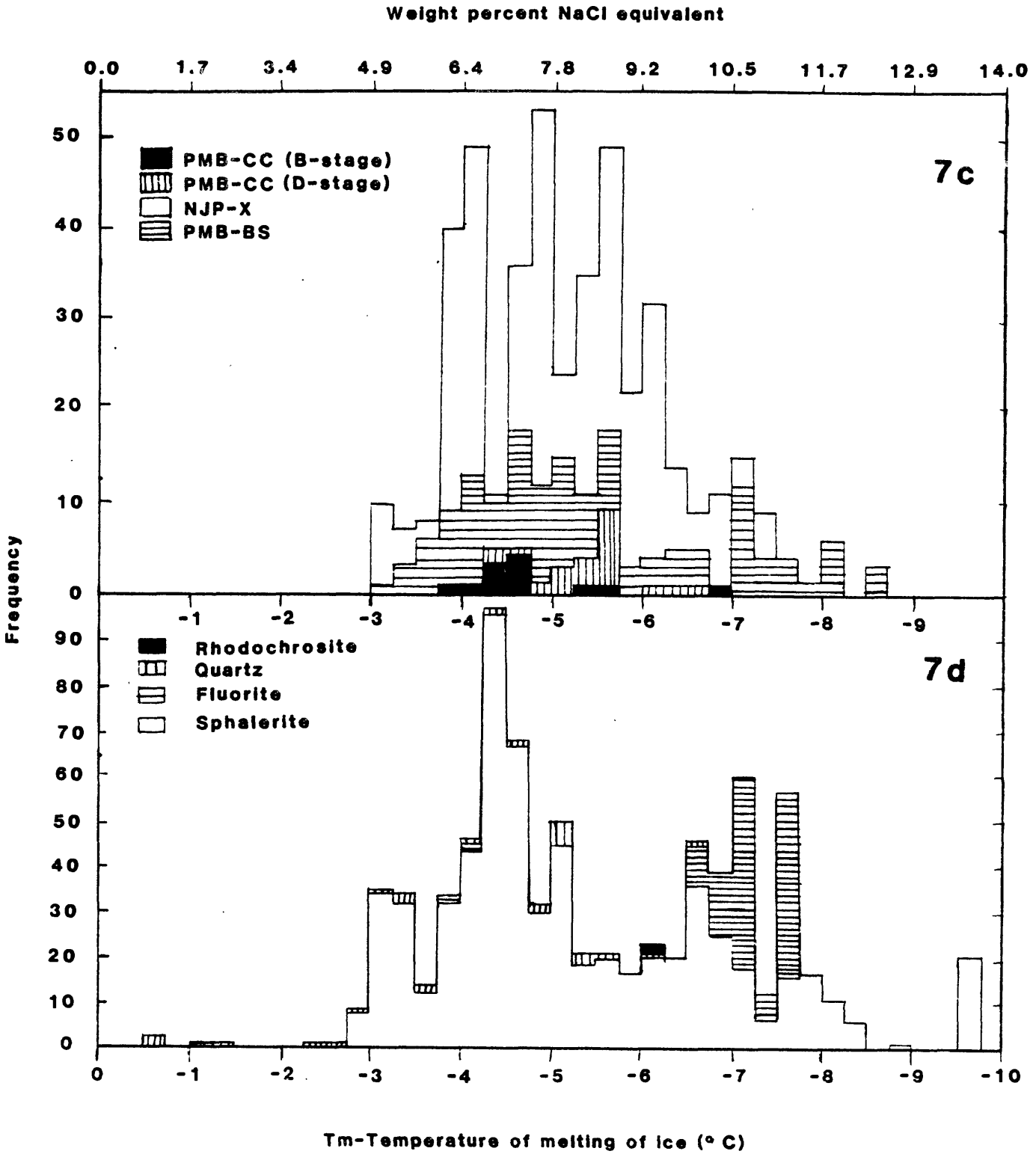
Weight percent NaCl equivalent
0.0
1.7
3.4
4.9
6.4
7.8
9.2
10.5
11.7
12.9
14.0
PMB-CC (B-stage)
PMB-CC (D-stage)
NJP-X
PMB-BS
7c
Frequency
Rhodochrosite
Quartz
Fluorite
Sphalerite
7d
Tm-Temperature of melting of ice (° C)

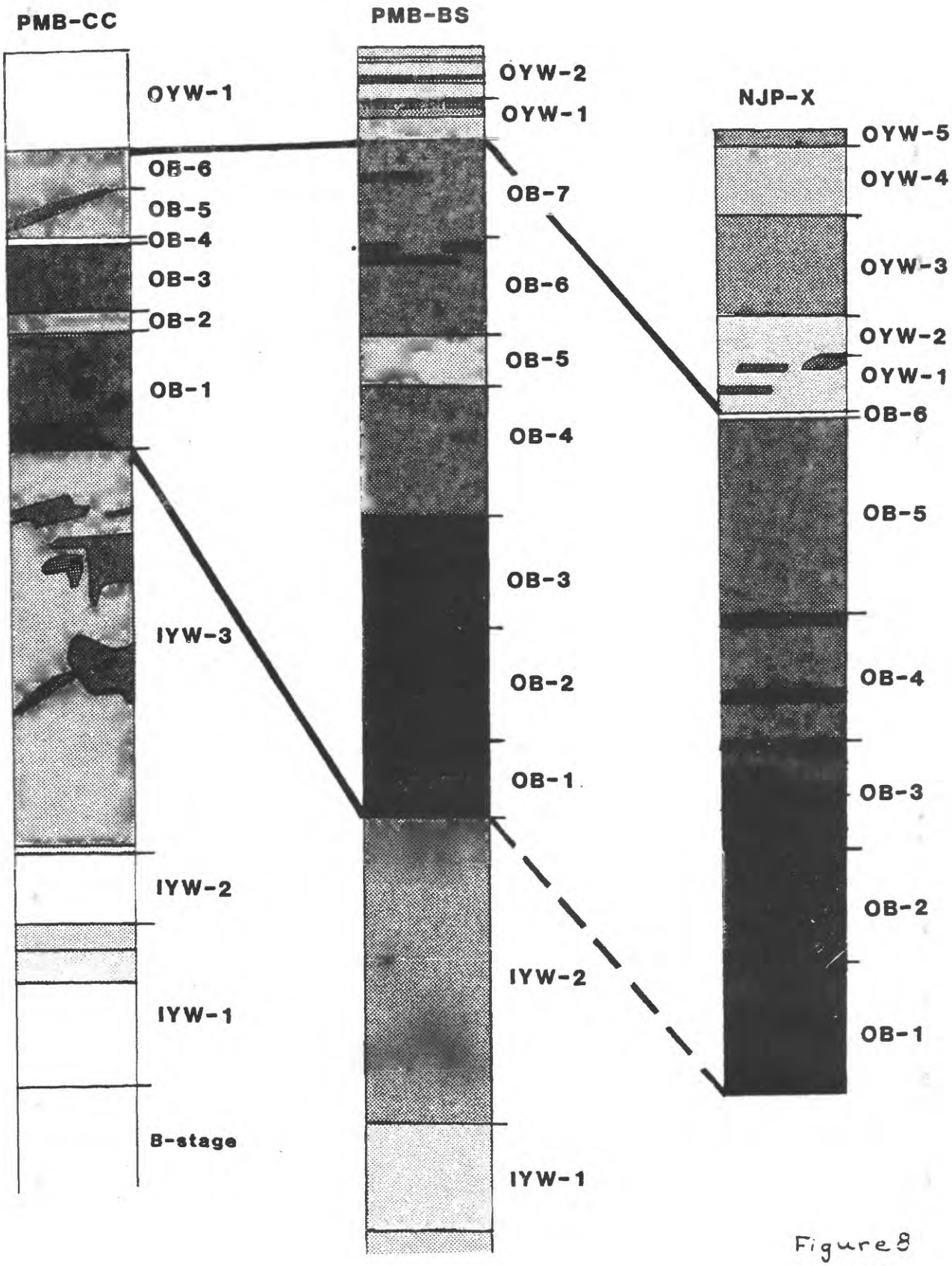
PMB-CC
OYW-1
OB-6
OB-5
OB-4
OB-3
OB-2
OB-1
IYW-3
IYW-2
IYW-1
B-stage
PMB-BS
OYW-2
OYW-1
OB-7
OB-6
OB-5
OB-4
OB-3
OB-2
OB-1
IYW-2
IYW-1
NJP-X
OYW-5
OYW-4
OYW-3
OYW-2
OYW-1
OB-6
OB-5
OB-4
OB-3
OB-2
OB-1

Figure 8

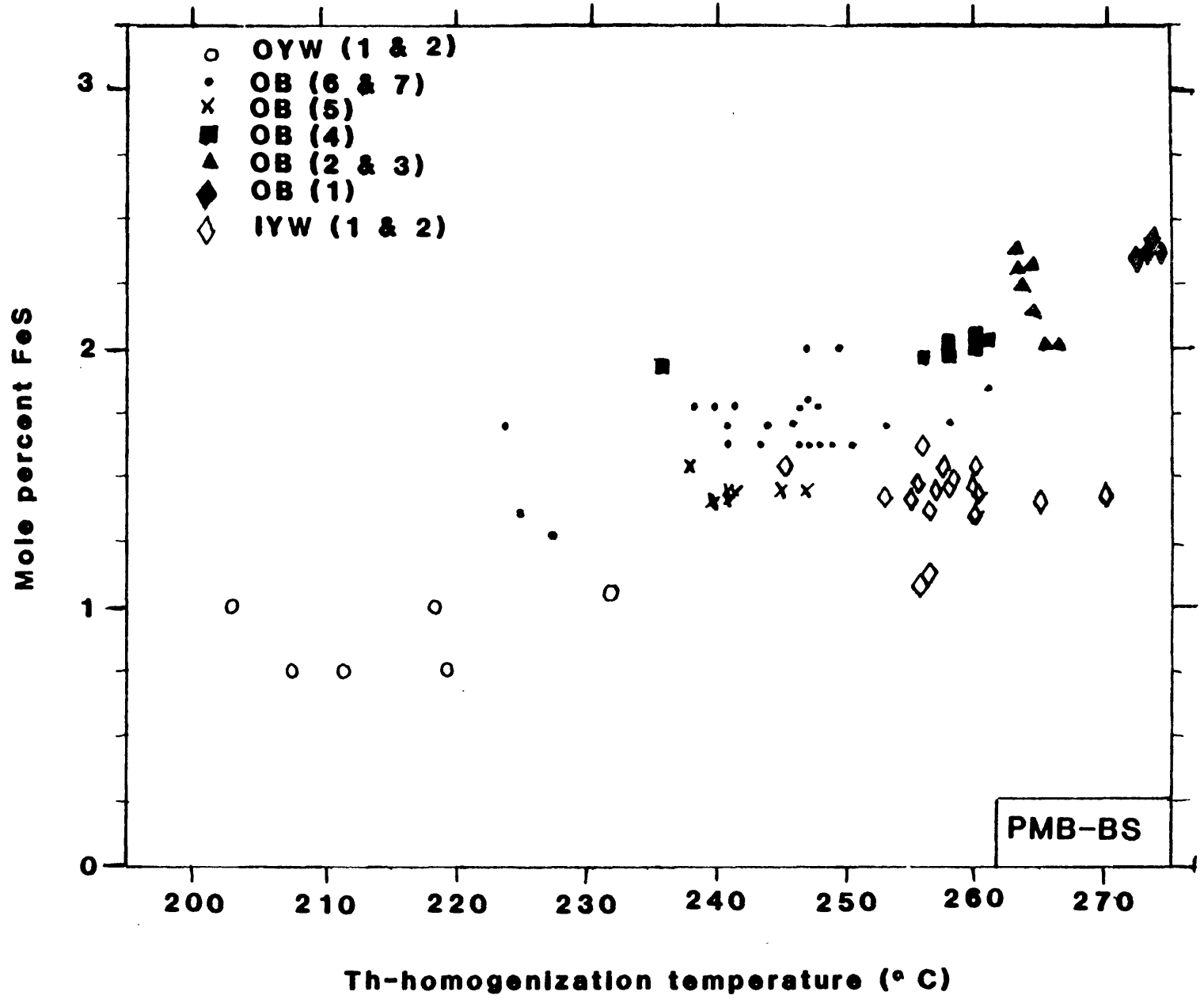
OYW (1 & 2)
OB (6 & 7)
OB (5)
OB (4)
OB (2 & 3)
OB (1)
IYW (1 & 2)
PMB-BS
Mole percent FeS
Th-homogenization temperature (° C)
0
1
2
3
200
210
220
230
240
250
260
270

Figure 9a

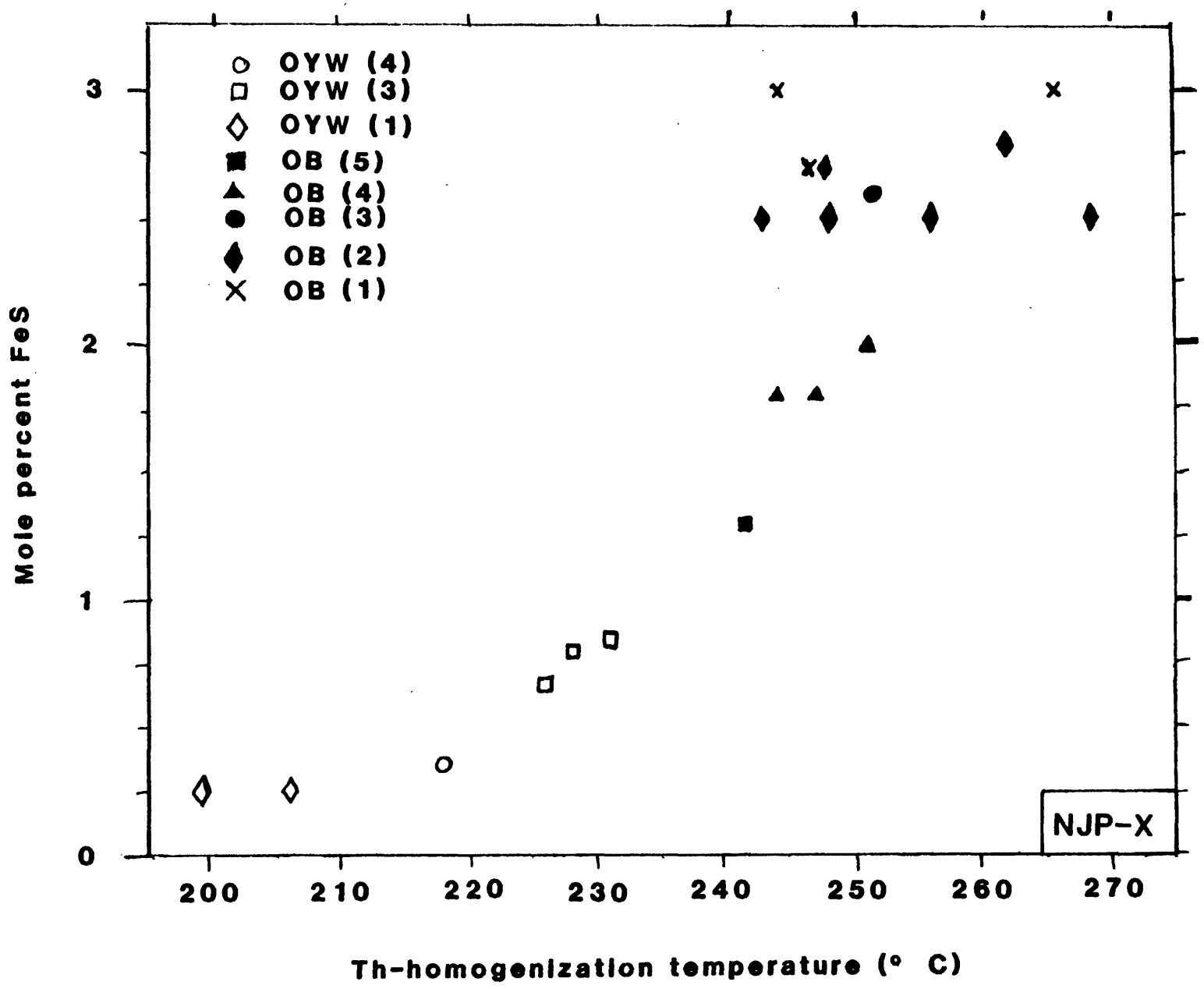
OYW (4)
OYW (3)
OYW (1)
OB (5)
OB (4)
OB (3)
OB (2)
OB (1)
NJP-X
Mole percent FeS
0
1
2
3
200
210
220
230
240
250
260
270
Th-homogenization temperature (° C)

Figure 9b

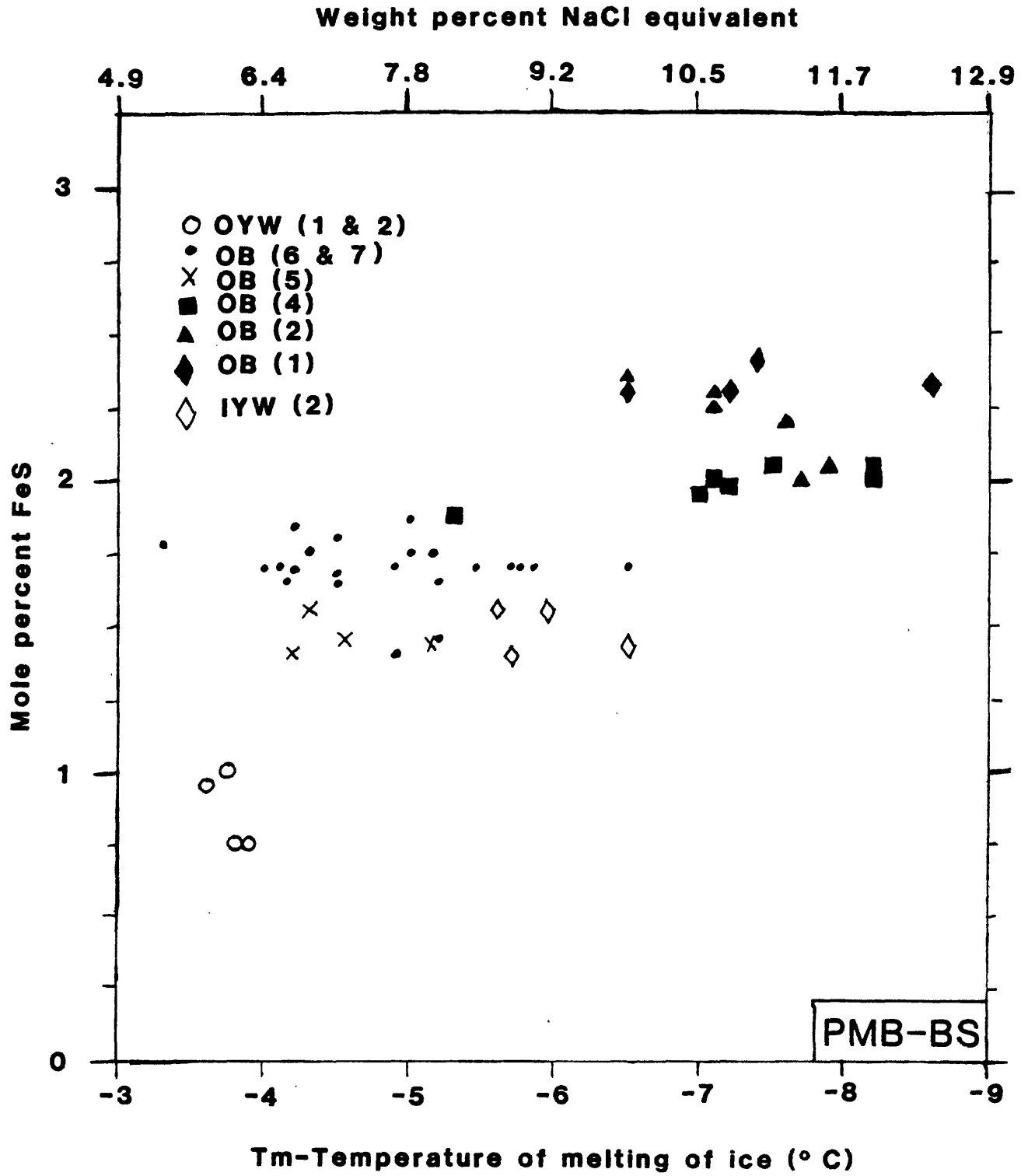
Weight percent NaCl equivalent
4.9
6.4
7.8
9.2
10.5
11.7
12.9
3
2
1
0
Mole percent FeS
OYW (1 & 2)
OB (6 & 7)
OB (5)
OB (4)
OB (2)
OB (1)
IYW (2)
PMB-BS
-3
-4
-5
-6
-7
-8
-9
Tm-Temperature of melting of ice (° C)

Figure 9c

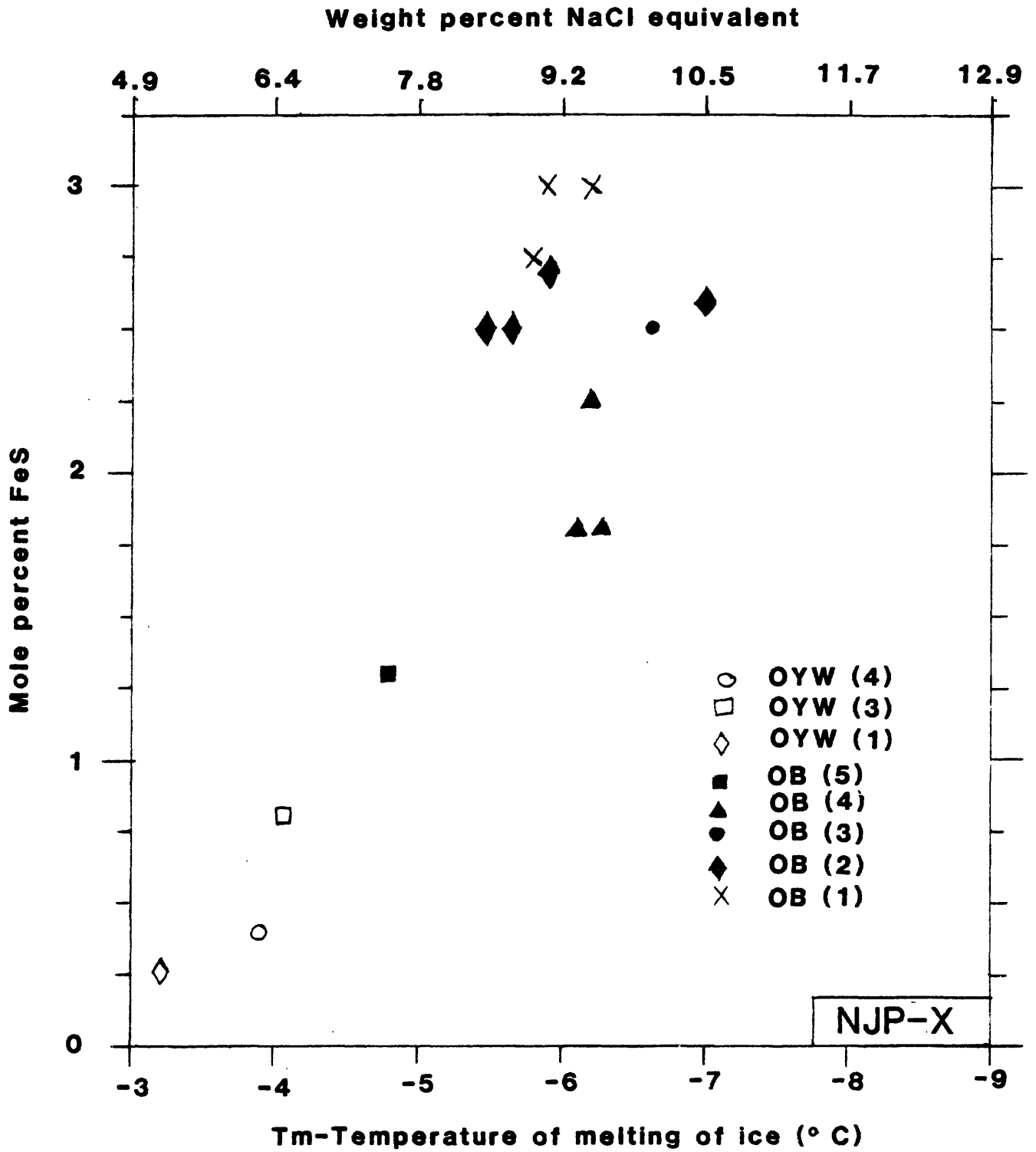
Weight percent NaCl equivalent
4.9
6.4
7.8
9.2
10.5
11.7
12.9
3
2
1
0
Mole percent FeS
OYW (4)
OYW (3)
OYW (1)
OB (5)
OB (4)
OB (3)
OB (2)
OB (1)
NJP-X
-3
-4
-5
-6
-7
-8
-9
Tm-Temperature of melting of ice (° C)

Figure 9d

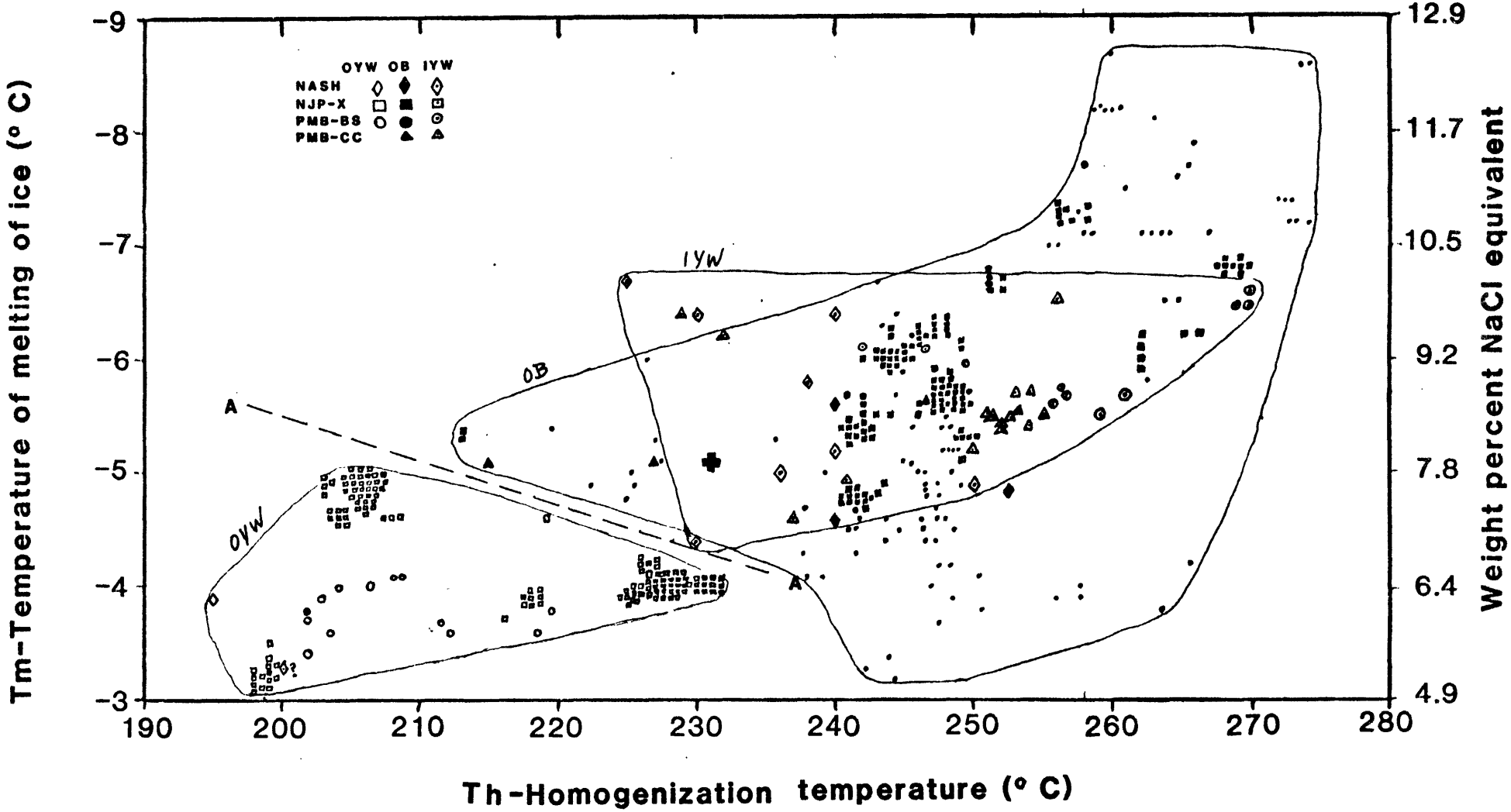
OYW OB IYW
NASH
NJP-X
PMB-BS
PMB-CC
IYW
OB
OYW
A
A'
-9
-8
-7
-6
-5
-4
-3
12.9
11.7
10.5
9.2
7.8
6.4
4.9
190
200
210
220
230
240
250
260
270
280
Tm-Temperature of melting of ice (° C)
Weight percent NaCl equivalent
Th-Homogenization temperature (° C)

Figure 10

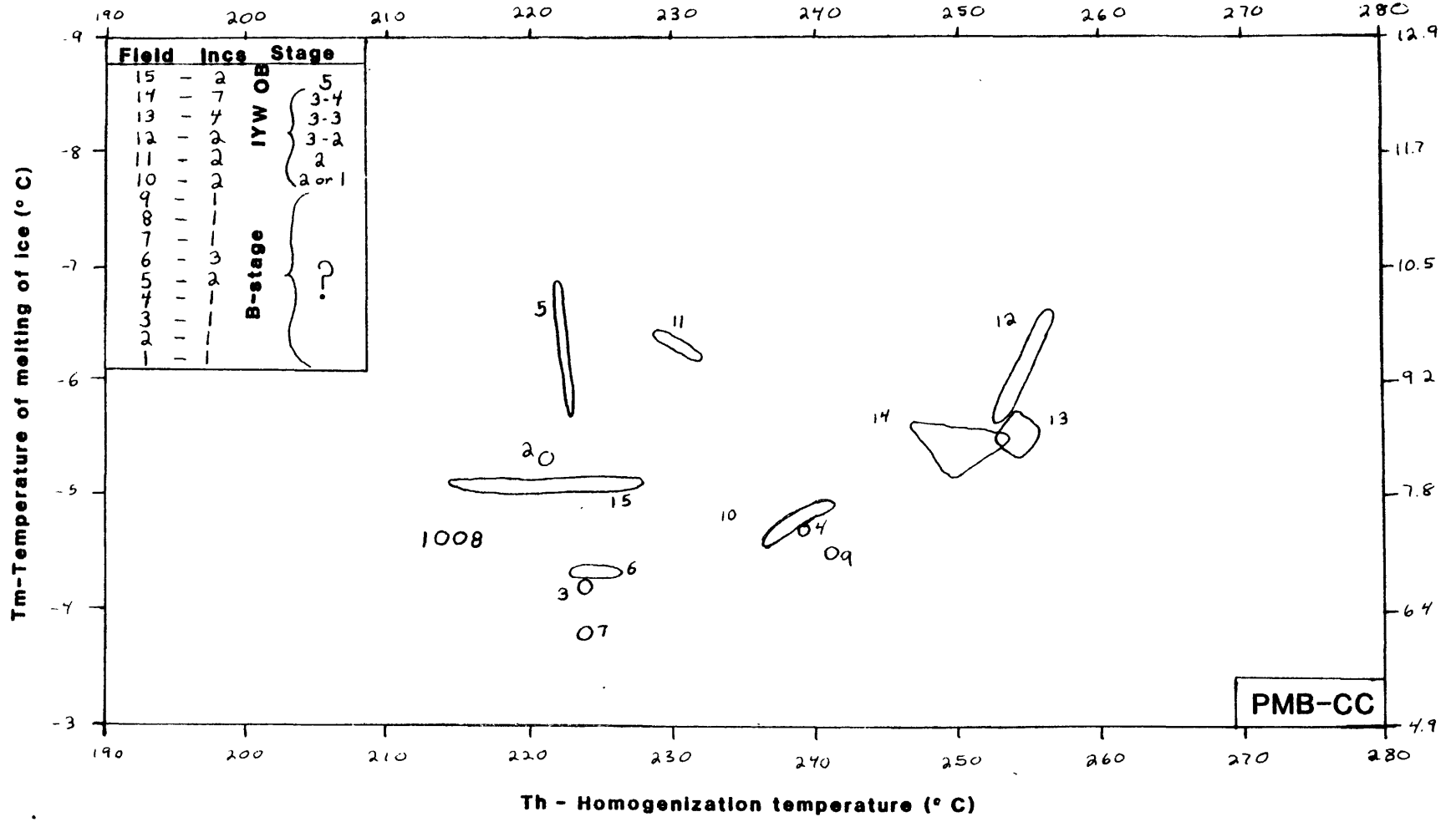
Field Incs Stage
15 – 2
14 – 7
13 – 4
12 – 2
11 – 2
10 – 2
9 – 1
8 – 1
7 – 1
6 – 3
5 – 2
4 – 1
3 – 1
2 – 1
1 – 1
IYW OB
5
3-4
3-3
3-2
2
2 or 1
B-stage
?
1008
PMB-CC
Tm-Temperature of melting of ice (° C)
Th - Homogenization temperature (° C)
Weight percent NaCl equivalent
190
200
210
220
230
240
250
260
270
280
-9
-8
-7
-6
-5
-4
-3
12.9
11.7
10.5
9.2
7.8
6.4
4.9

Figure 11a

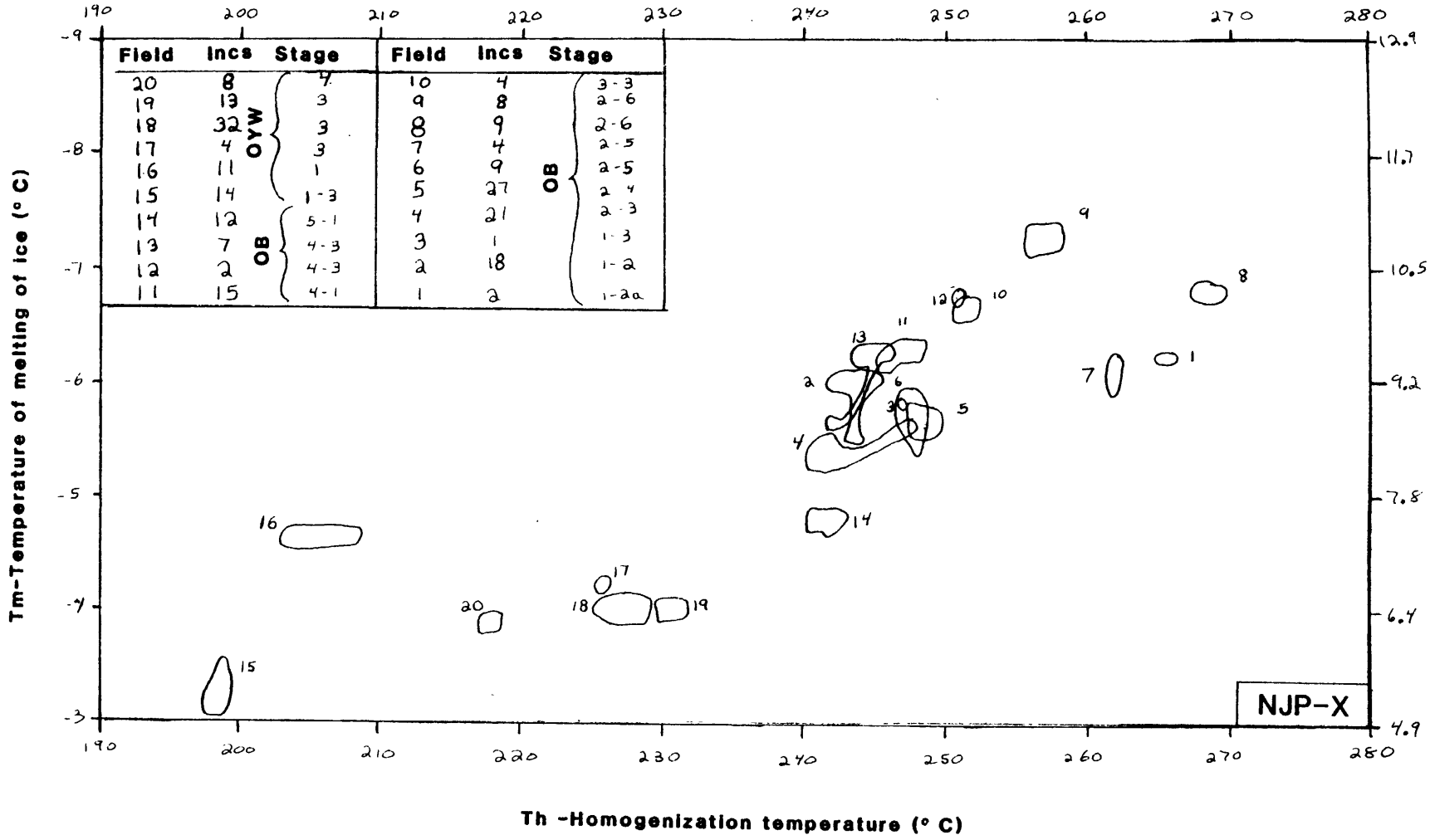
Field Incs Stage
20 8 4
19 13 3
18 32 OYW 3
17 4 3
16 11 1
15 14 1-3
14 12 5-1
13 7 OB 4-3
12 2 4-3
11 15 4-1
Field Incs Stage
10 4 3-3
9 8 2-6
8 9 2-6
7 4 2-5
6 9 OB 2-5
5 27 2 4
4 21 2-3
3 1 1-3
2 18 1-2
1 2 1-2a
NJP-X
Tm-Temperature of melting of ice (° C)
Th -Homogenization temperature (° C)
190 200 210 220 230 240 250 260 270 280
-9 -8 -7 -6 -5 -4 -3
12.9 11.7 10.5 9.2 7.8 6.4 4.9

Figure 11b

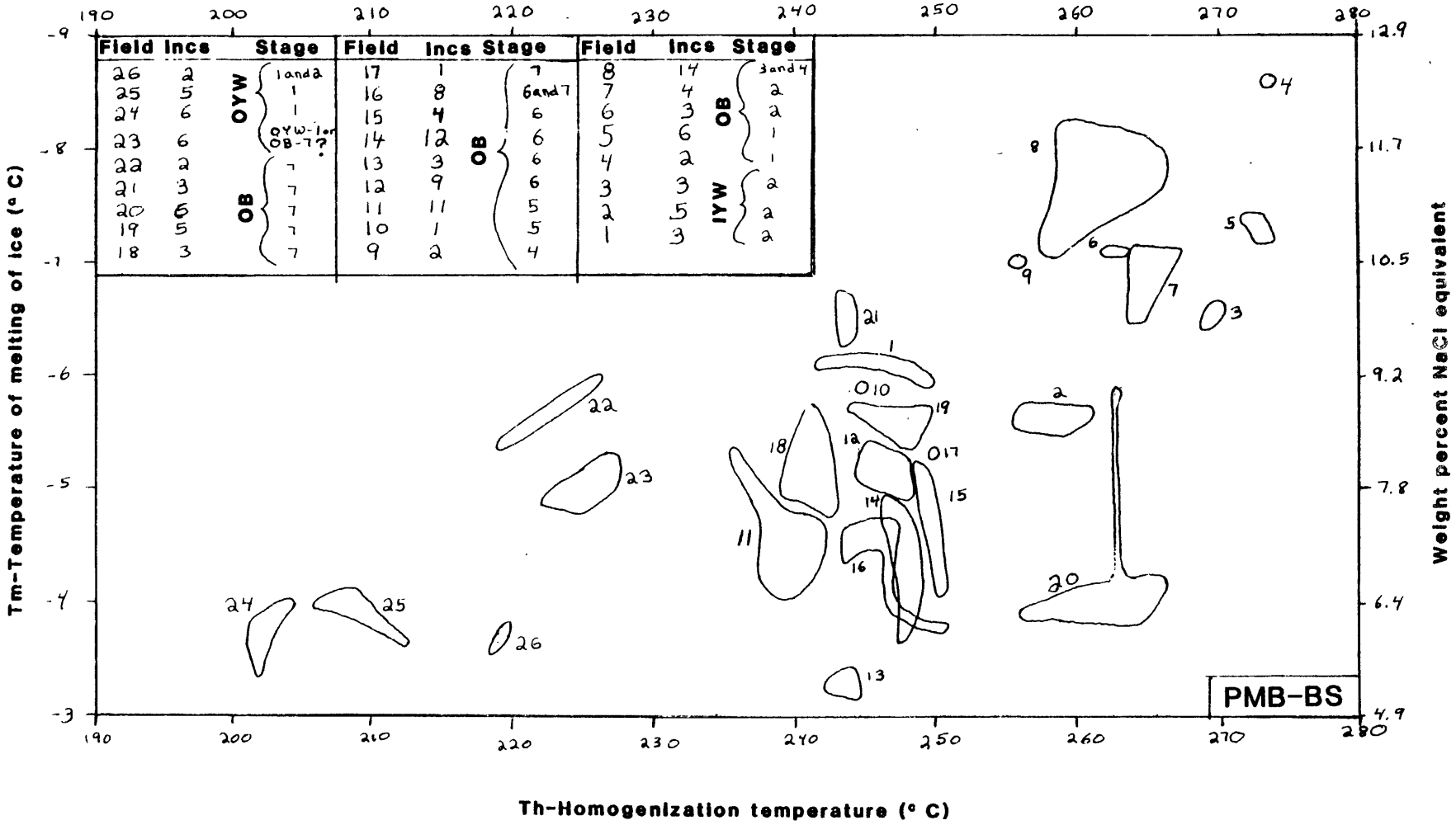
Field Incs Stage
26 2 OYW 1 and 2
25 5 OYW 1
24 6 OYW 1
23 6 OYW-1 or OB-1?
22 2 OB 1
21 3 OB 1
20 6 OB 1
19 5 OB 1
18 3 OB 1
Field Incs Stage
17 1 OB 7
16 8 OB 6 and 7
15 4 OB 6
14 12 OB 6
13 3 OB 6
12 9 OB 6
11 11 OB 5
10 1 OB 5
9 2 OB 4
Field Incs Stage
8 14 OB 3 and 4
7 4 OB 2
6 3 OB 2
5 6 OB 1
4 2 OB 1
3 3 IYW 2
2 5 IYW 2
1 3 IYW 2
PMB-BS
Tm-Temperature of melting of ice (° C)
Th-Homogenization temperature (° C)
Weight percent NaCl equivalent
190
200
210
220
230
240
250
260
270
280
-9
-8
-7
-6
-5
-4
-3
12.9
11.7
10.5
9.2
7.8
6.4
4.9

Figure 11c

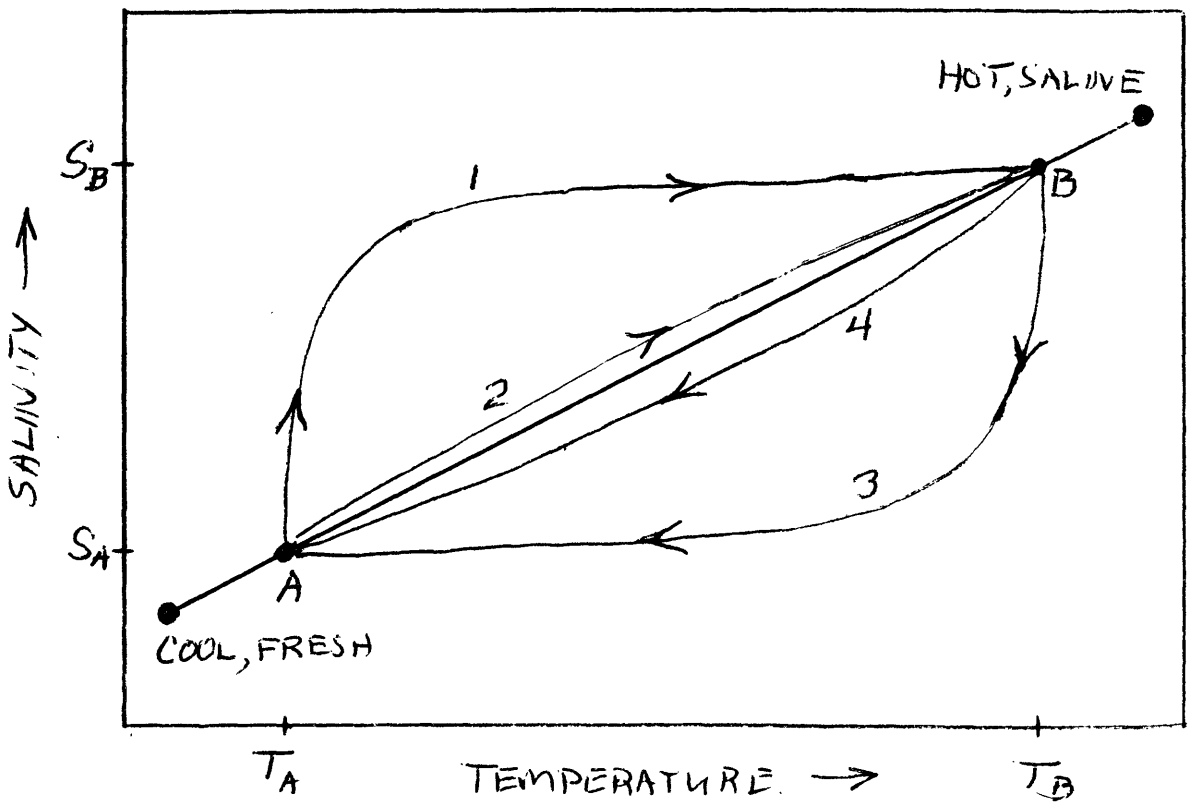
HOT, SALINE
S_B
B
1
4
2
3
S_A
A
COOL, FRESH
SALINITY →
T_A
TEMPERATURE →
T_B

Fig. 12